Research Square

Preprints are preliminary reports that have not undergone peer review.
They should not be considered conclusive, used to inform clinical practice,
or referenced by the media as validated information.

Expanding seaweed farming poses new risks to the ozone layer

Julia Velletta
School of Earth and Ocean Sciences, University of Victoria
Julian Villamayor
Institute of Physical Chemistry Blas Cabrera, CSIC https://orcid.org/0000-0002-8844-7389
Rafael Fernandez
Institute for Interdisciplinary Science (ICB), National Research Council (CONICET), FCEN-UNCuyo
Jennifer McHenry
University of Victoria
Carlos Cuevas
Institute of Physical Chemistry Blas Cabrera, CSIC
Maria Gasset
Institute of Physical Chemistry Blas Cabrera, CSIC https://orcid.org/0000-0001-6436-4055
Michael Sigmond
Environment and Climate Change Canada (ECCC) https://orcid.org/0000-0003-2191-9756
Julia Baum
University of Victoria https://orcid.org/0000-0002-9827-1612
Anoop Mahajan
anoop@tropmet.res.in
Indian Institute of Tropical Meteorology, Ministry of Earth Sciences, Pune, India https://orcid.org/0000-0002-2909-5432
Alfonso Saiz-Lopez
Institute of Physical Chemistry Blas Cabrera, CSIC https://orcid.org/0000-0002-0060-1581

Article

Keywords:

Posted Date: August 27th, 2026

DOI: https://doi.org/10.21203/rs.3.rs-10524078/v1

License: This work is licensed under a Creative Commons Attribution 4.0 International License.
Read Full License

Additional Declarations: There is **NO** Competing Interest.

Expanding seaweed farming poses new risks to the ozone layer

Julia Velletta[1,2]†, Julián Villamayor[3]†, Rafael Fernandez[4], Jennifer McHenry[5], Carlos A. Cuevas[3], Maria Gasset[6], Michael Sigmond[2], Julia K. Baum[5], Anoop S. Mahajan[7]* and Alfonso Saiz-Lopez[3]*

[1] School of Earth and Ocean Sciences, University of Victoria, Victoria BC, V8P 5C2, Canada.

[2] Environment and Climate Change Canada (ECCC); Victoria BC, V8N 1V8, Canada.

[3] Department of Atmospheric Chemistry and Climate, Institute of Physical Chemistry Blas Cabrera (CSIC); 28006 Madrid, Spain.

[4] Institute for Interdisciplinary Science (ICB), National Research Council (CONICET), FCEN-UNCuyo; 5501 Mendoza, Argentina.

[5] Department of Biology, University of Victoria; Victoria BC, V8P 5C2, Canada.

[6] Department of Biological Physical Chemistry, Institute of Physical Chemistry Blas Cabrera (CSIC); 28006 Madrid, Spain.

[7] Centre for Climate Change Research, Indian Institute of Tropical Meteorology, Ministry of Earth Sciences; Pune, 411008, India.

† These authors contributed equally to this work.

*Corresponding authors. Email: a.saiz@csic.es; anoop@tropmet.res.in

Abstract:

Seaweed farming is widely promoted for climate change mitigation[1,2], yet its potential unintended consequences on the stratospheric ozone layer via emissions of ozone-depleting short-lived halogens[3,4] is seldom acknowledged and remains unquantified. Applying newly developed observations-based seaweed-farming emission scenarios to a state-of-the-art Earth system model[5], reveals substantial global ozone depletion and increased surface shortwave radiation in the latter half of this century. Expansion of seaweed farming is projected to lead to Antarctic ozone declining below the historical minimum by the 2060s under 20% annual growth and by the 2090s under 12% annual growth, while a business-as-usual 6% annual growth would still substantially slow down ozone recovery. These findings serve as a warning that seaweed farming at scales proposed for global sustainability targets could pose a serious unintended risk to the ozone layer.

Main Text:

Seaweed farming is gaining attention globally as a strategy for climate change mitigation due to the ability of seaweed to sequester and store atmospheric and marine carbon[2,6–11]. Beyond their contributions to carbon cycling, seaweed play important ecological roles in marine ecosystems and support the production of a wide range of ecosystem goods and services, including food, feed, medicine, cosmetics, biostimulants, bioplastics, textiles, construction materials, and bioenergy. In a world of limited resources and concurrent environmental crises, several studies[1,10,12] have suggested the expansion of seaweed production as an opportunity to accommodate a growing human population in accordance with the United Nations Sustainable Development Goals[13]. As a result, global seaweed production has grown and is expected to further grow in the coming decades, driven by numerous plans to rapidly expand cultivation into new regions and applications[10,14–20]. Natural seaweeds predominantly grow in shallow coastal waters from the intertidal zone to depths exceeding 50 meters[21]. Given their ecological importance, efforts to conserve and restore natural seaweed habitats have intensified, particularly amid growing environmental challenges such as more frequent extreme weather events, rising ocean temperatures, and the spread of pests and diseases[22–24]. In parallel, farmed seaweed production, much of which can be cultivated offshore, has expanded considerably in recent decades (Extended Data Fig. 1), and there is widespread interest in further upscaling for both climate and socio-economic benefits[1].

Despite differences in assumptions and constraints, independent studies consistently highlight the considerable potential for expanding seaweed farming[25–27]. To date, global seaweed production, which was just over 35 million tons of fresh weight (MtFW) in 2023, remains well below the estimated global farming capacity. Although competition for nutrients and suitable temperature regimes limit the ocean area that is viable for seaweed cultivation, potential yields of about 700 gigatons of fresh weight per year (GtFW yr^{-1}) have been estimated within exclusive economic zones (EEZs)[1,25]. However, large-scale seaweed farming may also cause unintended environmental impacts, including nutrient depletion, competition with wild species and entanglement risks for marine wildlife[28,29]. To date, assessments of widespread seaweed farming expansion have largely focused on ecosystem- and resource-based impacts, while potential atmospheric consequences, particularly those related to emissions of ozone-depleting short-lived halogens (SLHs), have received comparatively little attention.

Along with phytoplankton, seaweed are well-known as major natural sources of ozone-depleting SLHs in the atmosphere, especially bromoform ($CHBr_3$) and dibromomethane (CH_2Br_2)[30–32]. They produce and release these halogenated compounds in response to environmental stress such as strong radiation, grazing, microbes, oxidation stress, or changes in temperature, salinity, and acidity[4,31,33]. Although present-day SLH emissions from seaweed are relatively small, projected extensive future farming and climate change are expected to greatly increase these emissions[34–37]. Once in the atmosphere, SLHs and their product gases exert complex direct and indirect climate effects[3,38], including the efficient destruction of stratospheric ozone[39–42]. The stratospheric ozone

layer is essential for shielding life from harmful solar ultraviolet radiation at the surface, and its depletion poses well-documented risks to human health and ecosystems[43–47]. For example, SLH-induced loss of lower stratospheric ozone has a major influence on the Earth's shielding from UV radiation[39,48]. Since the discovery of the Antarctic ozone hole[49] and the rapid implementation of the Montreal Protocol and its amendments[43,50], the stratospheric ozone layer has shown signs of recovery following the phase-out of regulated long-lived industrial ozone-depleting substances (ODS)[51–54]. However, while ODS emissions have declined and are subject to strict controls, the increasing, unregulated emissions of SLH associated with expanding seaweed farming remain largely overlooked.

In this study we use a comprehensive Earth system model to quantify the potential risks posed by enhanced SLH emissions associated with the expansion of seaweed production, as currently advocated, for the ozone layer. These results are enabled by the SLH and seaweed-farming emissions scenarios developed in this work, which allow us to explore how impacts on ozone intensify with industry growth. We show that ozone depletion increases as seaweed farming expands, ranging from a measurable weakening of ozone-layer recovery under business-as-usual growth to substantial depletion under accelerated expansion pathways.

SLH emissions from past and future seaweed farming

Quantifying the global atmospheric impacts of seaweed farming requires knowledge of the associated SLH emissions, which are currently lacking. To overcome this challenge, we develop new emission inventories by combining biomass data with species-specific release rates (see Methods). Available measurements of release rates vary widely among and even within seaweed genera due to interspecific differences among species and environmental influences (Fig. 1; see "Short-lived halogen (SLH) release rates from seaweed" in Methods). As a result, any given biomass value corresponds to a range of possible emissions, represented here by lower-range (25th percentile) and upper-range (75th percentile) estimates of release rates (Fig. 2).

For $CHBr_3$ alone, emissions from seaweed harvested before 2000 account for less than 1% (0.16-0.88%, corresponding to the lower-to-upper-range release rate estimates) of the estimated global total emission of 505 gigagrams of bromine per year (Gg Br yr^{-1})[55]. Since then, global seaweed harvest has increased at about 6% yr^{-1} (Extended Data Fig. 2), adding an estimated 24.5 MtFW between 2000 and 2020[56]. This additional biomass is estimated to have released 3.0-12.0 Gg Br yr^{-1} of $CHBr_3$ and 0.1-0.7 Gg Br yr^{-1} of CH_2Br_2 globally (Extended Data Fig. 3). Since these recent increases remain small relative to global background emissions (about 0.5-2.2%), any associated atmospheric signal would likely be too small to be robustly detected with current observational methods. This is due to the lack of sustained long-term atmospheric measurements of $CHBr_3$ and CH_2Br_2, particularly in coastal regions where seaweed-related changes are expected to be strongest. Consistently, previous studies and assessments[43,57–59] report no substantial long-term trends in these atmospheric bromocarbon abundances, reinforcing that any recent-past contribution from expanding seaweed production remains below current observational sensitivity.

If seaweed production continues to grow at its business-as-usual rate of 6% yr^{-1}, by 2050 there would be enough seaweed to feed a global population of nearly 9.7 billion assuming Japanese consumption levels (5.3 grams dry weight per person per day[1,60]). Under the 6% scenario, the resulting biomass in 2050 would lead to substantially larger $CHBr_3$ emissions of 23-92 Gg Br yr^{-1} and additional CH_2Br_2 emissions of 0.6-4.6 Gg Br yr^{-1}. If sustained through to the end of the century, this 6% yr^{-1} growth rate would produce added emissions roughly one to three times the current global total (Fig. 1b,c, green shading). However, for mitigation and sustainability pathways under a blue-economy framework, seaweed production is being promoted at a rate well above the historical 6% yr^{-1} [1,19]. A hypothetical but postulated 12% yr^{-1} growth scenario[1], representing a doubling of the current global growth rate, would produce over five times the seaweed biomass and associated SLH emissions in 2050 compared with the 6% yr^{-1} trajectory. Under the accelerated production scenario, sustained 12% yr^{-1} growth would increase global seaweed production by nearly an order of magnitude by the end of the century compared to 2020. Even so, projected seaweed production under 12% yr^{-1} scenario remains well below (less than half) the estimated aquaculture potential within EEZs. Furthermore, a "maximum", yet unlikely, scenario with a potential annual growth rate of 20% yr^{-1} would approach an upper limit to seaweed farming, reaching approximately 700 GtFW yr^{-1} by 2077. Under this scenario, estimated emissions span about 72-280 teragrams of bromine per year (Tg Br yr^{-1}) from $CHBr_3$, plus 2-13 Tg Br yr^{-1} from CH_2Br_2, while the combined bromine emissions sum to 133 Tg Br yr^{-1} based on the median release rate estimate.

Impact on the ozone layer

To quantify the potential impacts of seaweed farming on the ozone layer over the course of the 21st century, we prescribe the projected emissions of seaweed-derived SLHs in the Community Earth System Model with interactive SLH chemistry (CESM2-SLH)[5]. First, we perform a reference simulation spanning the 1960–2000 historical period and extending to 2099, assuming no expansion in seaweed farming, i.e., no additional seaweed emissions beyond the background[55]. Our evaluation of model performance indicates that CESM2-SLH is capable of reproducing key observed features of upper-stratospheric inorganic bromine (Br_y) and total ozone column (TOC), consistent with previous observational assessments (see "Model validation" in Methods; figs. S6–S7). The evolution of Antarctic ozone in the reference simulation captures both the October minimum in TOC around 2004 and the subsequent recovery (Fig. 3). Under these baseline conditions, October TOC averaged over 90–60°S returns to 1980 reference values by the late 2050s, in line with previous multi-model assessments[43,61] (Extended Data Fig. 7).

Next, we conduct a set of simulations in which SLH emissions increase from 2000 to 2020 following estimated historical seaweed emissions, and onward following predicted annual growth rates in seaweed production of 6%, 12%, and 20%, representing a range of future expansion pathways as described above. Incorporating these distinct seaweed-growth scenarios markedly alters the reference trajectory, progressively buffering and ultimately reversing the projected Antarctic ozone recovery (Fig. 3).

Under the lowest seaweed farming growth rate considered, the business-as-usual 6% yr^{-1} scenario, the ozone recovery remains close to the baseline trajectory through mid-century. However, the recovery trend reverses toward the end of the century, buffering the projected Antarctic TOC recovery by ~25% in 2099 relative to the reference, i.e. without expanding seaweed farming. The more accelerated expansion scenario of 12% yr^{-1} produces a clear reversal of ozone recovery, with October Antarctic TOC falling below the historical minimum by 2092. Under the maximum expansion scenario of 20% yr^{-1}, the reversal is both much stronger and earlier: October TOC drops below the historical minimum already by 2067. After crossing this threshold, Antarctic ozone loss continues to intensify, reaching unprecedented low levels until seaweed farming approaches its estimated upper potential (around 2077 in the 20% yr^{-1} scenario; Fig. 2). At this point, the October TOC deficit is nearly twice the magnitude of the historical ozone hole minimum around 2004 and expands far beyond the polar regions and into the global stratosphere.

Overall, these results reveal a pronounced sensitivity of future ozone to sustained seaweed expansion. Both the timing and the magnitude of the TOC deficit strongly depend on the seaweed farming growth rate, with higher growth rates driving an earlier crossing of the historical minimum and substantially larger long-term ozone loss. Unlike the historical Antarctic ozone hole, the ozone depletion driven by seaweed-derived SLHs is not confined to polar latitudes or to austral spring but expands toward mid-latitudes (see inset global projections in Fig. 3) and persists year-round (Extended Data Fig. 8). The annual-global mean ozone loss increases up to 17-fold in the high-end expansion pathway compared with the historical minimum baseline (-8.6 DU in 1996; Fig. 3), indicating a transition from a primarily regional and seasonal phenomenon to a global and year-round perturbation of the ozone layer.

The largest ozone depletion occurs in the lower stratosphere (below ~30 hPa down to the tropopause; Extended Data Fig. 9), where ozone changes strongly affect the Earth´s radiative balance[48,62]. Consistent with this vertical sensitivity, the ozone depletion-driven increase in surface downwelling shortwave radiation becomes far more geographically widespread than the historical Antarctic ozone hole (Fig. 4). In the reference simulation around 2004, the excess surface shortwave radiation relative to pre-ozone hole conditions (1960-1980) is largely confined to southern high latitudes: The annual mean ranges from ~0.5 W m^{-2} at 60º S to ~1.5 W m^{-2} at the South Pole, with negligible values northward of ~30º S (Fig. 4). In contrast, future seaweed expansion scenarios lead to a much broader geographical imprint. Under both the 12% yr^{-1} growth scenario in 2092 and the 20% yr^{-1} growth scenario in 2067, annual-mean excess shortwave radiation exceeds ~1.5 W m^{-2} poleward of ~40º latitude in both hemispheres, indicating that northern and southern mid-latitude regions experience year-round ozone-driven radiative perturbations comparable to those historically associated with the ozone hole in the Antarctic Circle during spring. Under the scenario with 20% yr^{-1} growth, the effect becomes global by the end of the century, with a global-mean annual shortwave radiation excess of 1.7 W m^{-2}. Values increase from 1.3 W m^{-2} near the equator to 2.8 and 3.0 W m^{-2} in the Arctic and Antarctic, respectively, thereby exceeding the historical maximum ozone depletion observed during Antarctic spring (90º - 60º S). These radiative effects extend well beyond polar regions into densely populated and biodiversity-rich mid-latitude areas, implying a substantial increase in potential

societal and ecological vulnerability to ozone-driven changes in surface ultraviolet and shortwave radiation[43–47].

Conclusions and Sectoral Implications for Seaweed Farming

By projecting the estimated SLH emissions from seaweed farming through the 21st century and simulating their atmospheric impacts, this work identifies these emissions as an unintended serious environmental risk to the ozone layer at the scales of industrial expansion currently being proposed within this century. Under rapid expansion scenarios (i.e., 12% and 20% yr^{-1} growth rates), the results indicate severe stratospheric ozone loss in the second half of this century, leading to unprecedented anomalies in the extra-polar ozone layer, exceeding the magnitude of ozone depletion during the peak Antarctic ozone hole period. In contrast to the historically localized and markedly seasonal Antarctic ozone hole, ozone loss driven by seaweed-derived SLHs emerges as a more persistent and increasingly global response, extending into midlatitudes and the lower stratosphere, where ozone changes exert a particularly strong influence on radiative balance. Consistent with this, high-end seaweed expansion scenarios produce a marked amplification of ozone loss and associated increases in surface downwelling shortwave radiation, with annual-mean excess values exceeding ~1.5 W m^{-2} across large areas of the midlatitudes and reaching a global-mean increase of ~1.7 W m^{-2} by the end of the century in the highest emission case (20% yr^{-1} growth). As a result, ozone-driven radiative perturbations extend well beyond polar regions into areas of high population density, pointing to a growing potential for societal and ecological risks associated with sustained large-scale seaweed harvest development.

At business-as-usual 6% yr^{-1} growth rates, the effects appear relatively modest until approximately 2075, though are predicted to slowly reverse the Antarctic recovery if seaweed production growth is maintained afterwards. Regardless of how fast growth occurs, ozone layer concentrations level off and decline once SLH emissions exceed approximately two to three times the present-day background levels of 505 Gg Br yr^{-1} (roughly equivalent to harvesting 3.5-5 GtFW, depending on the efficiency of $CHBr_3$ and CH_2Br_2 production by individual seaweed species)[3]. Furthermore, even under the 6% yr^{-1} growth scenario, the impact on total stratospheric bromine reaching the ozone layer is substantial: global mean upper-stratospheric bromine decreases from ~22.4 pptv in the early 2000s to 13.9 pptv by 2099 in the reference case with no seaweed emissions, but only to 20.8 pptv under 6% yr^{-1} growth (Extended Data Fig. 6). This implies that approximately 81% of the bromine-related recovery achieved under the Montreal Protocol would be effectively offset by the end of the century. Besides, note that bromine is about 60 times more efficient at destroying ozone than chlorine from long-lived ODS[3]. Taken together, these results indicate that sustained expansion along seemingly moderate growth pathways would also ultimately lead to severe ozone losses in addition to those projected under faster expansion scenarios.

The impact on ozone estimates presented here may indeed be a conservative estimate for several reasons. First, the SLH emissions used, although based on broad assumptions, also lie on the conservative side: We considered the increase of only the two dominant SLHs, while it is known that seaweed emits a variety of other ozone-depleting halocarbons including bromine-, chlorine-,

and iodine containing species[3,4] not considered in this study. Furthermore, we assumed that farms use a static future seaweed species blend mirroring recent seaweed harvest records, whereas industry-driven shifts toward stronger emitters like *Asparagopsis spp,* could substantially elevate total emissions[34,63]. Even if the species cultivated in future seaweed farming remain the same as at present, increasing climate change related stressors, such as heat stress, shifts in salinity, oxidation stress and grazing, are likely to cause higher overall SLH release and emissions[36,64], with uncertain consequences from climate-driven redistribution of target species[65]. Second, this study used one Shared Socioeconomic Pathway, namely SSP3-7.0, in which carbon dioxide (CO_2) and methane (CH_4) rise faster than in a more moderate scenario, such as SSP2-4.5. Within CMIP6 models, SSP3-7.0 produces higher baseline TOC by 2100 across most latitudes[61]. As a result, ozone depletion induced by seaweed-farming-enhanced SLH emissions occurs against an elevated TOC background, partially offsetting its apparent magnitude. In scenarios with weaker background ozone production (e.g., SSP2-4.5), the same SLH emissions from seaweed would lead to even lower absolute TOC levels than those projected here for SSP3-7.0.

Finally, while seaweed farming may offer a powerful tool in reducing and removing carbon from the atmosphere to fight climate change and in satisfying food demand to combat undernourishment, the unintended deleterious consequences for the ozone layer of continued expansion in seaweed farming call for careful reconsideration. A steady continuation of the current 6% yr^{-1} annual growth rate could remain broadly consistent with ozone layer recovery until the 2070s but can reverse the Antarctic recovery by the end of the century, and threatens the bromine reductions achieved by the Montreal Protocol. On the other hand, rapid growth scenarios such as 12–20% yr^{-1} could erode the global ozone layer to unprecedented minimum levels during the second half of the century. The findings indicate that future aquaculture practices must ensure that seaweed-derived SLH emissions do not exceed approximately two to three times present-day background levels, in order to prevent large-scale impacts on stratospheric ozone. Hence, strategic choices, such as selecting appropriate seaweed species and farming locations, become imperative to prevent or attenuate negative impacts, while extended monitoring and proactive research can guide policymakers to prioritize effective measures and safeguard against a potential new unintended environmental crisis.

Figures

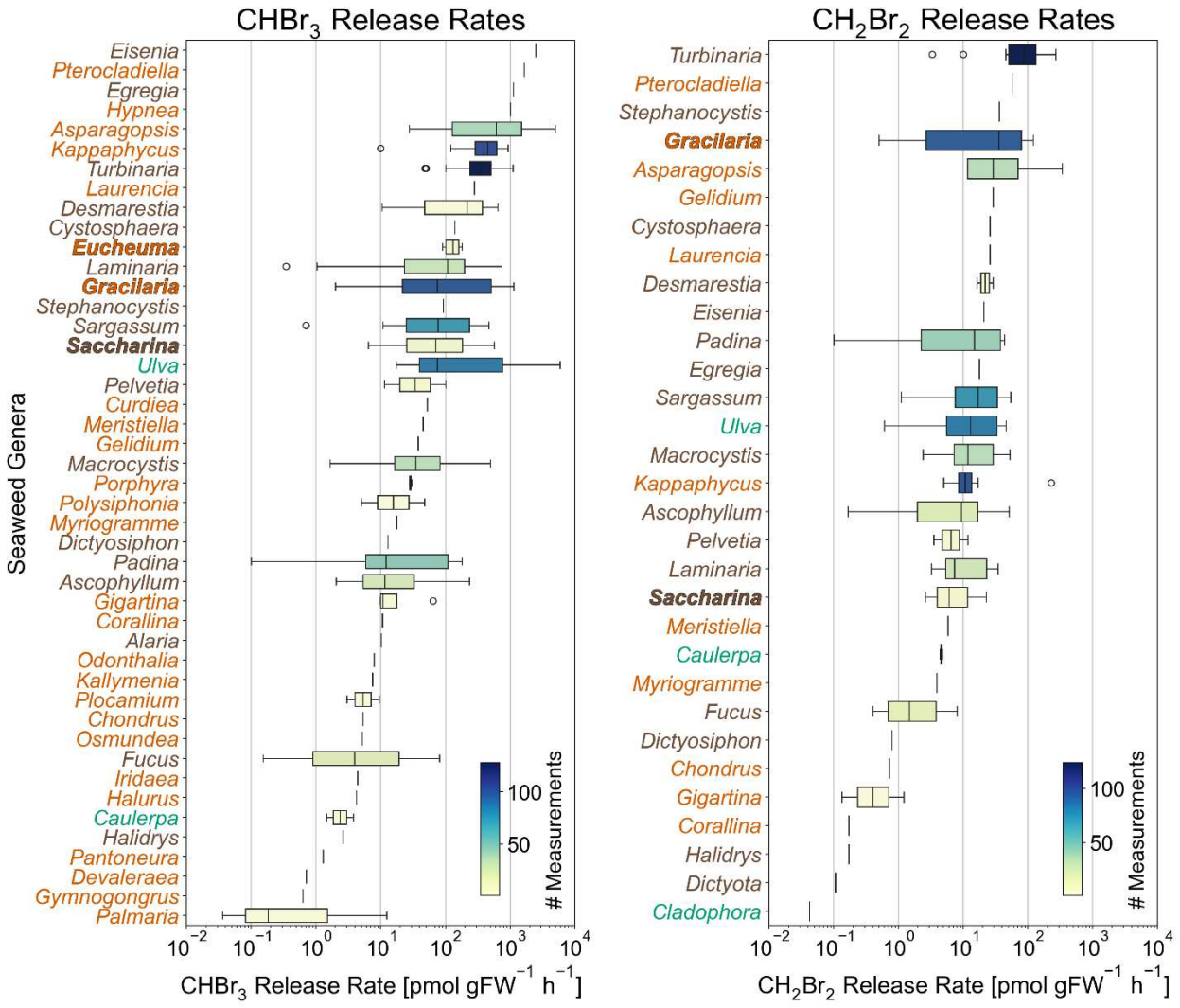


Fig. 1. Bromoform ($CHBr_3$) and Dibromomethane (CH_2Br_2) release rates vary among seaweed species and within species due to environmental factors. Seaweed genera (y-axis) are ranked by release rate median and colored by phyla: Rhodophyta (orange), Phaeophyceae (brown), and Chlorophyta (green). Seaweed genera contributing >10% to the global seaweed harvest in recent decades (*Saccharina*, *Eucheuma*, and *Gracilaria*) are displayed in bold font. Color shading indicates the total number of measurements reported in the literature for each genus. Box plots represent variability among study-level release rate estimates across conditions rather than population-level percentiles and may include multiple studies, experimental settings, and species.

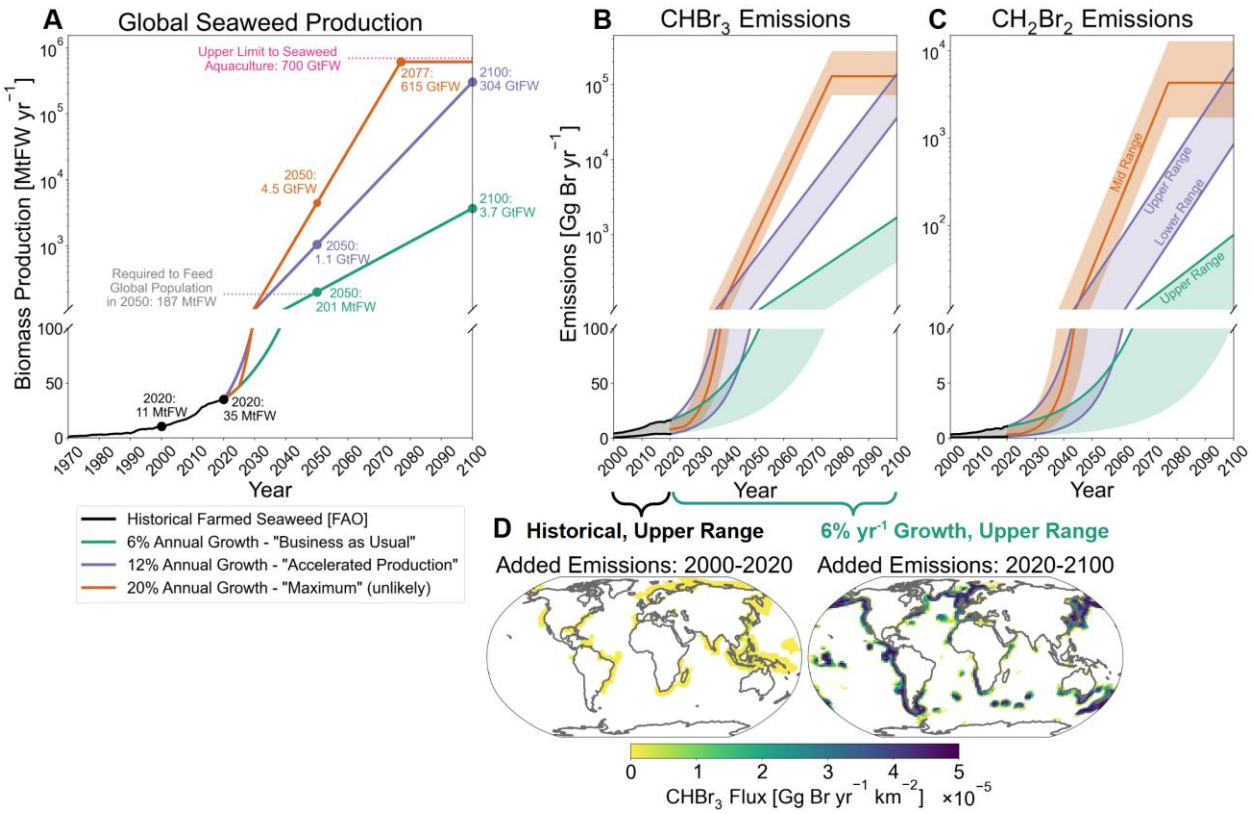
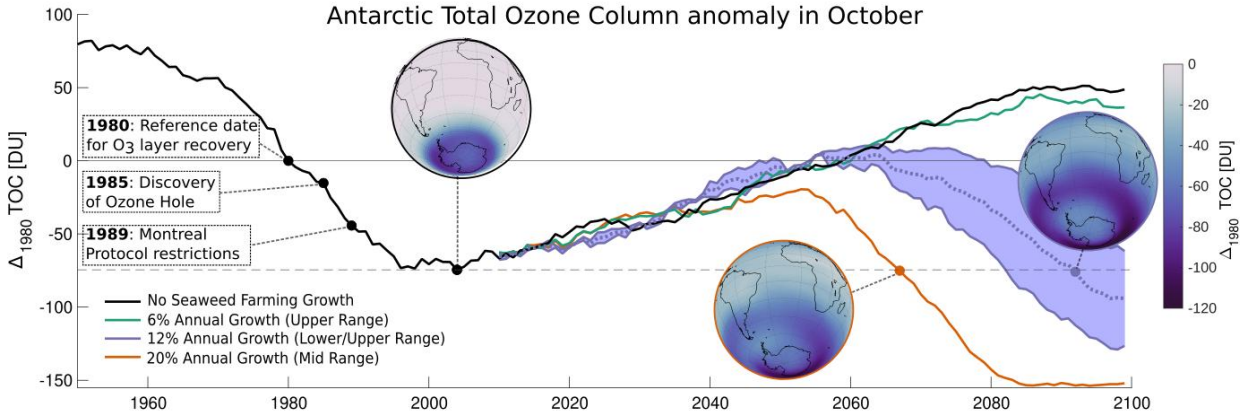


Fig. 2. Past and projected seaweed production with resulting $CHBr_3$ and CH_2Br_2 emissions. **(A)** Biomass of farmed seaweed harvest based on historical FAO records up to 2020, followed by three future scenarios representing different growth rates, and the associated **(B)** $CHBr_3$ and **(C)** CH_2Br_2 emissions range using lower- and upper-range release rate estimates. Model experiments were conducted for the four emissions scenarios represented by the solid lines in (B) and (C). Note that the y-axis is split, with a linear scale at the bottom and a logarithmic scale at the top to show the detail for earlier years, while capturing the magnitude of later growth. **(D)** Added emissions between 2000 and 2020, and between 2020 and 2100 for the 6% yr^{-1} growth rate scenario with the upper-range release rate estimate.



286

287 **Fig. 3. Modeled evolution of the Antarctic ozone hole and the projected impact of seaweed**
288 **farming.** Time series of October mean total ozone column (TOC) anomalies averaged over 90º -
289 60º S relative to 1980. Colored lines denote seaweed production growth scenarios initiated in 2020
290 and projected to 2099 (see legend); the black line denotes the benchmark simulation starting in
291 1960 without growing seaweed emissions considered (black line). All timeseries are smoothed
292 with an 11-year centered running mean to highlight long-term trends. Inset globes show polar
293 views of the 11-year mean TOC anomalies centered on the historical minimum (i.e., maximum
294 Antarctic ozone hole; 2004) and on the years when October Antarctic TOC returns to that
295 minimum (horizontal dashed line): 2067 for the median 20% yr^{-1} growth scenario and 2092 for
296 the mean of the two 12% yr^{-1} growth simulations**.**
297

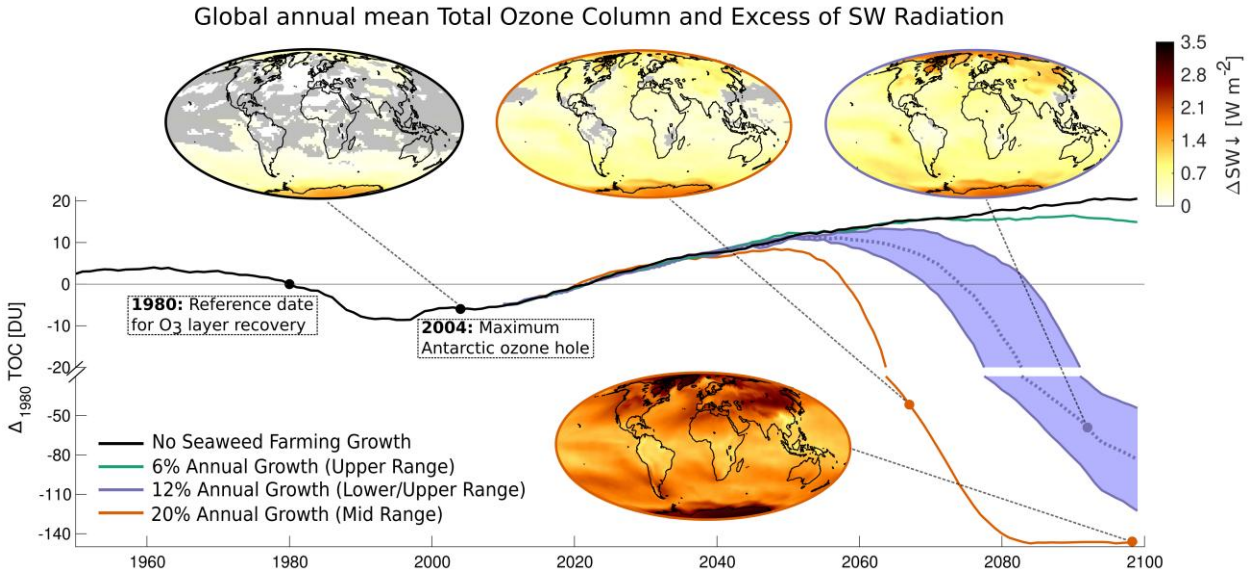


Fig. 4. Projected impact of seaweed farming on the global ozone layer and associated surface radiative effects. Time series as in Fig. 2, but for global- and annual-mean total ozone column (TOC) anomalies (relative to 1980). The y-axis is split into different scales to show the detail of the variability in the past and the conservative and moderate projections of seaweed farming development while also capturing large deviations in the late-century high-emission scenarios. Maps show the 11-year mean ozone-driven excess in surface downwelling shortwave radiation ($\Delta SW_{\downarrow}^{O3}$) relative to 1960-1980, centered on 2004 (the modeled historical minimum of October Antarctic TOC; Fig 2), on 2067 for the median 20% yr^{-1} growth scenario and on 2092 for the mean of the two 12% yr^{-1} growth simulations (the years when October Antarctic TOC returns to 2004 minimum level; Fig 2), and on 2099 for the median 20% yr^{-1} growth scenario. Gray shading marks regions where $\Delta SW_{\downarrow}^{O3}$ is not statistically significant (Methods).

Methods

Past and future global seaweed production

Estimating global seaweed production from cultivation and farming is challenging as standing biomass reflects the balance between concurrent gains and losses, dynamics that are shaped by intrinsic biological rates (e.g., primary production, growth, and reproduction), extrinsic pressures (e.g., disease, herbivory, and physical abrasion), and biophysical conditions (e.g., nutrient availability and wave exposure)[66]. Socioeconomic conditions (e.g., capital investment, infrastructure, governance and regulatory quality) also play a role in determining the scale of production[67,68]. While live biomass can be estimated using remote sensing and imaging, selective sampling, and models that balance gain and loss terms over time considering different for environmental factors, the resulting approximations have varying levels of uncertainty locally due to the differing quality and availability of data across the globe[69–71].

The best available biomass estimates for globally harvested seaweed production come from direct measurements collated by the Food and Agriculture Organization (FAO), which maintains a comprehensive dataset on the annual seaweed harvests by countries worldwide[56]. Harvested biomass primarily originates from farmed seaweeds, with small quantities also from wild-collected natural seaweed stands (Extended Data Fig. 1). During seaweed cultivation, some biomass is lost from grazing, pests, and disease, or intentionally left unharvested for further growth or reproduction. Hence, the harvested amount represents only a portion of the cultivated biomass, albeit likely the largest one.

Over past decades cultivated seaweed harvest reported by the FAO[56] increased on an average annual rate of slightly above 6% yr^{-1} globally (Extended Data Fig. 2). In view of the recent growth in seaweed cultivation and the promoted future growth[1], we project total global biomass through the end of the century using three scenarios: (a) "business as usual", reflecting a continuation of the historical 6% yr^{-1} growth; (b) "accelerated production", representing a hypothetical but postulated doubling of the historical global growth rate to 12% yr^{-1}, consistent with sustainability-oriented blue-economy ambitions[1], and (c) a "maximum" highly unlikely, but also postulated, case scenario consisting in a 20% yr^{-1} growth rate from 2026, preceded by a growth rate of 6% yr^{-1} from 2021 to 2025. All of these growth rates have been discussed in Duarte et al.[1] as viable and desirable scenarios until 2050; this study continues their projection until the end of the century (Fig. 1). In 2078, the 20% yr^{-1} growth rate scenario would exceed an upper limit of 700 gigatons of fresh weight per year (GtFW yr^{-1}) for seaweed production within exclusive economic zones (EEZs)[25]. Therefore, the biomass harvest is set to plateau before reaching this threshold, stabilizing at 615 GtFW yr^{-1} in 2077. It should be noted that the potential seaweed production would be even higher if cultivation was permitted beyond EEZ boundaries.

Global potential for seaweed farming

The ocean surface is vast, yet environmental constraints such as competition for nutrients and suitable temperature regimes limit the area viable for seaweed farming. Nonetheless, the EEZ provides about 48 million km^2 [25], with a potential yield of about 700 GtFW yr^{-1} [1]. Considering stricter socio-economic constraints (including considerations for depth, port distance, shipping traffic, marine protected areas, etc.), Spillias et al.[27] estimates still a substantial 6.5 million km^2 suitable for seaweed farming, equivalent to roughly 65-650 GtFW yr^{-1} when assuming average yields of between 1,000-10,000 tons dry weight (DW) km^2 yr^{-1}. For comparison, the 2023

production provided over 35 million tons of fresh weight (MtFW) harvest cultivated on approximately 2,500 km² [26] and wild seaweed occupies an area of about 6 million km² [1].
Allowing for open-ocean farming beyond the EEZ, Wu et al.[72] estimated a feasible potential of almost 70 million km², while Spillias et al.[27] modelled 119 million km², and Arzeno-Soltero et al.[26] projected up to 130 million km². Despite variations in these estimates depending on underlying assumptions and considerations, all studies agree that significant expansion of seaweed farming is feasible.
While global seaweed production in the past was primarily driven by China and other Asian countries[56], future seaweed farming is likely to expand into new regions, including American and European coastal waters[66]. To avoid making assumptions about the spatial distribution of future seaweed production, which will depend on complex socio-economic drivers and climate change evolution, we distribute the projected global seaweed biomass after 2020 uniformly across the area identified as suitable for seaweed cultivation in the "Limited Nitrate Scenario" by Arzeno-Soltero et al.[26]. Because this scenario explicitly limits seaweed productivity to nitrate naturally replenished from depth, it provides a conservative, biophysically grounded basis for distributing projected biomass under large-scale cultivation conditions. While that analysis considers the seaweed farming potential over the whole ocean, we further restrict the potential cultivation area to national Exclusive Economic Zones (EEZs), yielding a more conservative estimate of the potential expansion area suggested in the above-mentioned studies, namely, about 37 million km^2.

Short-lived halogen (SLH) release rates from seaweed

We compiled SLH release measurements from existing phycology literature. The dataset summarizes 23 studies[4,30,31,33,34,73–90] and covers release rates from 76 macroalgae species for up to 15 SLH (e.g., $CHBr_3$, CH_2Br_2, CH_2I_2, CH_3I, CH_2BrI, $CHBr_2Cl$) with varying amounts of data available within groups of seaweed. Bromoform ($CHBr_3$) typically exhibits the highest release rates and has the most abundant data available, followed by dibromomethane (CH_2Br_2) while data for the other minor SLHs is sparse. Therefore, and supported by the fact that CHBr3 and CH2Br2 are the two major SLHs contributing to stratospheric bromine loading[43,57,91], in this study we focus on presenting results for $CHBr_3$ and CH_2Br_2.

All observations from literature were standardized to a common unit of picomoles per gram of seaweed fresh weight per hour (pmol gFW^{-1} h^{-1}). Where the original measurements were reported on a dry-weight basis, conversion to fresh (wet) weight was required. In such cases, we used dry-to-fresh weight ratios reported in the same study whenever available. When study-specific conversion factors were not provided, we relied on average ratios derived from the literature for the corresponding seaweed group. These ratios were assigned by systematically prioritizing available data from progressively broader taxonomic levels, beginning at the species level and escalating to genus, family, order, and finally phyla.

Data on SLH release rates are sparse and heterogeneous across studies, with variability in experimental design, environmental conditions, and reporting practices. We extracted the available reported release rate values, treating each as a distinct observation corresponding to a specific experimental condition. Reported values include means or medians derived from varying numbers of measurements. However, to prevent over-representing individual conditions with higher replication, all extracted values were treated equally in the synthesis. In Fig. 1, we summarized variability across studies and conditions using box plots, which reflect the spread of reported values rather than statistically inferred population distributions. Color shading of the boxplots represents the cumulative number of individual measurements underlying those estimates aggregated across studies. For example, a box plot based on six reported study-level values may

be colored to reflect a larger total number of measurements if each study includes multiple replicate measurements. As such, resulting quartiles should be interpreted as descriptive ranges representing variability across experimental and environmental contexts, rather than confidence intervals or pooled population percentiles. These quartile values were subsequently used to define lower-range (25^{th} percentile), mid-range (median), and upper-range (75^{th} percentile) emission scenarios, providing a span that captures inter-study and inter-condition variability in reported release rates.

The large spread in SLH release rates within seaweed taxonomic groups (Fig. 1) can also be attributed to differences in seaweed species, environmental conditions, and measurement practices, data availability and uncertainties[4,80,84]. The highest release rates were usually measured during conditions of environmental stress[83,92]. $CHBr_3$ release rates are especially high from *Asparagopsis spp.*, a seaweed that is gaining attention for its capacity to reduce methane emissions from livestock[63,93]. There are few genera with even higher release rates, however, their limited data warrants caution regarding the reliability of these values (Fig. 1). The three most commonly cultivated seaweeds genera, i.e., *Saccharina, Eucheuma*, and *Gracilaria*, account for roughly two-thirds of the global harvest and exhibit average release rates of approximately 100 pmol $CHBr_3$ gFW^{-1} h^{-1} and 10 pmol CH_2Br_2 gFW^{-1} h^{-1} (Extended Data Fig. 4C).

Estimating SLH emissions

In this study, we utilize the aforementioned FAO cultivated biomass data[56] and multiply it with the average SLH release rates of the reported seaweed genera to estimate recent past SLH emissions resulting solely from harvested farmed seaweed. This approach assumes that all SLH released from algae tissue completely outgas into the atmosphere without any oceanic loss—an assumption considered reasonable by previous studies[34,84]. Given the additional biomass portions from unaccounted cultivated seaweeds and natural stands, as well as the omission of SLH release for the minor species contributing to ozone depletion, it is important to note that our total SLH emission estimates from seaweed are conservative.

We use the $CHBr_3$ and CH_2Br_2 emissions by Ordóñez et al.[55] as a reference dataset and consider this dataset to be valid up to the year 2000, before seaweed farming significantly began to contribute to global emissions. The Ordóñez et al.[55] halocarbon emissions inventory has been validated with essentially all available global short-lived halocarbon observational datasets and it is widely used by most global chemistry-climate models that include halogen chemistry. This reference dataset includes seasonal variability but assumes constant annual emissions sources of ~505 gigagrams of bromine per year (Gg Br yr^{-1}) from $CHBr_3$ and ~62 Gg Br yr^{-1} from CH_2Br_2. We assume that the minor contributions of SLH emissions from farmed seaweed prior to 2000 (<1% for $CHBr_3$) are already included in that inventory, while emissions after 2000 are treated as incremental. Accordingly, relative post-2000 increases in seaweed emissions were added to the reference dataset. Added SLH emissions after 2000 and before 2020 are calculated for each country's annual seaweed harvest, as detailed in the FAO records. Since different countries have cultivated various types of seaweed over time, past global SLH emissions are not directly proportional to the total seaweed biomass, but depend on the average SLH release rates of the specific seaweed mix each year.

Since seaweed species can have wide ranges of release rates (Fig. 1), for the given biomass harvested by a country, we use the lower-range and upper-range estimates of the $CHBr_3$ and CH_2Br_2 release rates from each country's seaweed mix to estimate a range of resulting emissions for each year between 2000 and 2020. For example, in 2016, Indonesia produced 9.7 MtFW of *Eucheuma* and 1.4 MtFW of *Gracilaria*. Using the lower-range release rate estimate for *Gracilaria* (25 pmol gFW^{-1} h^{-1} for $CHBr_3$), we estimate partial emissions of 0.065 Gg Br yr^{-1}, while the upper-

range release-rate estimate (537 pmol gFW^{-1} h^{-1} for $CHBr_3$) yields partial emissions of 1.526 Gg Br yr^{-1}. Similarly, for *Eucheuma*, we estimate the lower-range emissions to be 2.177 Gg Br yr^{-1} based on the release rate estimate of 101 pmol gFW^{-1} h^{-1}, and upper-range emissions of 3.438 Gg Br yr^{-1} based on the release rate estimate of 160 pmol gFW^{-1} h^{-1}. The combined $CHBr_3$ emissions from seaweed harvest in Indonesia in 2016 are therefore estimated to range between 2.243 and 4.965 Gg Br yr^{-1} and CH_2Br_2 emissions are derived following the same approach. Release rate measurements are not available for all seaweed species and compounds (e.g., no CH_2Br_2 release rates are reported for *Eucheuma*). In such cases, release rates from the next highest available taxonomic level are applied, hierarchically considering species, genus, family, order, and ultimately phylum, in order to maximize data coverage while maintaining taxonomic consistency.

Each country's added $CHBr_3$ and CH_2Br_2 emissions are converted into fluxes (in molecules per second per centimeter^2) over its corresponding EEZ and added to the reference. Past $CHBr_3$ and CH_2Br_2 emissions from seaweed harvest have predominantly originated from China, followed by Indonesia, the Philippines, and South Korea (Extended Data Fig. 3). After 2020, we extended the dataset until the end of the century using the three growth-rate scenarios described above under "Past and Future Global Seaweed Production". Future SLH emissions depend on the release rates of the farmed seaweed species. For simplicity, we assume that the types of seaweed under cultivation remain broadly comparable over time. From 2010 to 2020, *Saccharina, Eucheuma,* and *Gracilaria* together comprised about two-thirds of the biomass produced globally (see pie chart in Extended Data Fig. 4b). Using the average blend of harvested seaweeds from this recent period, we can calculate more robust statistical metrics of the average global SLH release rates, including mean and median values, and lower range and upper range estimates (see Table in Extended Data Fig. 4c). Historically, the composition of the global seaweed harvest varied over time (Extended Data Fig. 4a), and in the future, changing economic value may continue to shift the global mix of cultivated seaweed species. However, given the uncertainty surrounding future changes in species composition, we assume continuity in the cultivation of similar seaweed species as in the recent past. Consequently, the seaweed blend and average SLH release rates presented in Extended Data Fig. 4 are presumed to remain constant.

The $CHBr_3$ and CH_2Br_2 emissions after 2020 are computed as global totals and then converted to fluxes across areas suitable for seaweed cultivation, as modeled in the "Limited Nitrate Scenario" by Arzeno-Soltero et al.[26], but restricted to EEZs. In this study, we assume that this suitable cultivation area remains static through the end of the century, even though climate change may impact future production potential by altering species distribution. For example, the biome of wild temperate seaweed (e.g., kelp forests) is projected to undergo poleward range shifts and decline globally by approximately 15% under SSP3-7.0[23]. However, the suitable area for cultivated seaweed may be less vulnerable to climate change because farms can adapt through species substitution, selective breeding, and relocation to more favorable regions.

Time-slice examples of the $CHBr_3$ fluxes used to drive the model simulations are shown in Extended Data Fig. 5.

Model description and simulation setup

We used the Community Earth System Model version 2 with interactive SLH chemistry (CESM2-SLH)[5], employing the fully coupled chemistry-climate configuration in which the Whole Atmosphere Community Climate Model version 6 (WACCM6)[94] is coupled to the Parallel Ocean Program version 2 (POP2) oceanic model[95]. The simulations are based on the *BWHIST_slh* model configuration described in Fernandez et al.[5], featuring a high-top atmospheric setup with 70

vertical levels extending from the surface to 6×10^{-6} hPa (~140 km) and a horizontal resolution of 2° x 2° [5,94]. This high-top model configuration resolves stratospheric internal variability and a comprehensive gas-phase and heterogeneous chemistry scheme spanning the whole atmosphere[96]. A reference simulation was conducted for the period 1960–2099, following the Shared Socioeconomic Pathway 3-7.0 (SSP3-7.0)[97] for future gas emissions from 2015 onward, using the standard CESM2-SLH high-top configuration with comprehensive SLH chemistry[5]. The SSP3-7.0 scenario is characterized by rapidly increasing greenhouse gas concentrations and yields higher baseline total ozone column (TOC) values by the end of the century across most latitudes in state-of-the-art chemistry-climate models[61]. Consequently, projected ozone changes driven by SLH emissions in this scenario occur against a high ozone background, providing a conservative estimate of SLH-induced ozone loss relative to scenarios with lower greenhouse gas concentrations and lower baseline ozone levels.

The reference simulation includes oceanic emissions of SLH halocarbons (e.g., bromocarbons and iodocarbons) following the inventories of Ordóñez et al.[55], abiotic emissions of inorganic iodine (I_2 and HOI)[98], and halogen activation from sea-salt aerosol dehalogenation[38,99]. Anthropogenic SLH chlorocarbon compounds are included as described in Fernández et al.[5], using lower-boundary conditions for $CHCl_3$ and $C_2H_4Cl_2$, and surface emissions for CH_2Cl_2 and C_2Cl_4 based on Hossaini et al.[100] and Claxton et al.[101]. Natural oceanic SLH emissions, including $CHBr_3$ and CH_2Br_2 bromocarbons, exhibit prescribed latitudinal and seasonal variability that is repeated annually, implying constant background emissions from natural seaweed sources and neglecting long-term trends in natural seaweed distribution or future emissions related to seaweed farming.

In addition to the reference projection, we performed four future (2020–2099) sensitivity simulations in which incremental seaweed farming fluxes of $CHBr_3$ and CH_2Br_2, derived in this work, are prescribed. These include (i) the upper-range emission estimate for the "business as usual" growth scenario (6% yr^{-1}), (ii) the lower- and upper-range emission estimates for the "accelerated production" growth scenario (12% yr^{-1}), and (iii) the mid-range emission estimate for the "maximum" growth scenario (20% yr^{-1}).

Model validation

Model evaluation focused on the key atmospheric components relevant to this study, namely the response of stratospheric bromine to changes in SLH emissions and the comparison of simulated TOC with global and Antarctic observations during the historical period. Additional validation of the CESM2-SLH model is presented elsewhere[5].

First, we evaluated the transport of inorganic bromine (Br_y) into the upper stratosphere by comparing simulated global-mean Br_y at 3.5 hPa with corresponding estimates and observations reported in the World Meteorological Organization´s Scientific Assessment of Ozone Depletion: 2022[43] (Extended Data Fig. 6, inset). The close agreement in both the abundance of total Br_y and its historical trend supports a realistic representation of halogen transport and chemistry relevant for stratospheric ozone loss. We note that, unlike the WMO assessment which assumes fixed global additions of Br_y from SLH halocarbons of 5 ± 2 pptv (see inset in Extended Data Fig. 7), the CESM2-SLH configuration includes spatially and seasonally varying surface emissions of all halocarbons. This approach yields an additional present-day annual-mean bromine injection of 4.3-5.2 pptv[5].

We then assessed the simulated ozone response by comparing TOC anomalies relative to 1980 with satellite-based observational estimates from the Bodeker Scientific Filled Total Column Ozone Version 3.4 (BSFilledTCO v3.4) dataset[102] for the period 1979–2016, as well as with simulations from other state-of-the-art Coupled Model Intercomparison Project Phase 6 (CMIP6)

models[61]. For a consistent intercomparison, we selected only CMIP6 models that include interactive chemistry and were forced with the same SSP3-7.0 used here (*50*) (Extended Data Fig. 8). The reference simulation reproduces the observed low-frequency evolution of TOC anomalies (models smoothed with an 11-year centered running mean, observations unfiltered) in both Antarctic October (90°–60°S) and the global annual mean, and remains within the spread of the interactive-chemistry CMIP6 ensemble. Overall, these results support the suitability of CESM-SLH for assessing long-term ozone variability and its response to chemically driven forcings such as enhanced SLH emissions from seaweed farming.

Statistical significance of 11-year mean patterns

The global patterns shown in Fig. 4 represent the mean ozone-driven excess in surface downwelling shortwave radiation anomaly, calculated at each grid point using an 11-year window centered on the target year. The uncertainty associated with this mean was estimated from the 95% confidence interval (CI) of the mean, assuming a Student's t distribution:

$$CI = t_{0.025,\,N-1}\frac{\sigma}{\sqrt{N-1}},$$

w here $N = 11$ is the number of annual values included in the average, σ the standard deviation across the 11-year period and $t_{0.025,N-1}$ is the two-tailed critical t value for $N-1$ degrees of freedom. This significance assessment therefore identifies regions where simulated anomalies emerge above internal interannual variability in the model, rather than representing absolute detection limits in the real atmosphere.

Uncertainties and limitations

Additional targeted research would further refine and strengthen estimates of SLH emissions and thereby improve confidence in their representation in Earth system models. Uncertainties and limitations in the current body of knowledge necessitate a few well-motivated assumptions and approximations in our analysis.

Key sources of uncertainty in the estimation of SLH emissions relate to incomplete knowledge of:

- SLH release rates from different seaweed species, including how these rates vary with environmental conditions such as temperature, light availability, nutrients, and physiological stress;
- The behavior of SLH dissolved in seawater, including mixing, potential chemical transformation, and effective lifetimes, particularly under scenarios of elevated background oceanic SLH concentrations;
- Sea–air exchange processes for SLH, whose magnitude and controlling factors may vary with surface turbulence, stratification, and gas solubility under a changing climate; and
- The spatial distribution and species composition of seaweed biomass, both at present and in the future, as influenced by climate change, coastal development, socioeconomic factors, and the expansion of aquaculture.

Addressing these knowledge gaps would enable tighter constraints on SLH emission estimates and a narrower range of associated uncertainty. In particular, long-term atmospheric measurements

of SLH in coastal regions, especially in proximity to seaweed farming sites, would provide a critical observational basis to monitor emissions, characterize their variability, identify their trends, and support model evaluation.

Additional uncertainty arises from the reactive transport and pathways of individual SLH species emitted from different regions and latitudes. These processes depend on the strength of convective transport with respect to the large-scale ascent, as well as on species-specific photochemical lifetimes that vary with background atmospheric composition. Importantly, these controlling factors are themselves expected to evolve with global warming, highlighting the value of explicitly exploring their sensitivity in future work.

Building on the present analysis, future modeling efforts could prioritize the use of ensemble simulations to better constrain internal climate variability, explore multiple SSPs to assess climate change impacts, and test alternative spatial distributions of emissions. Such analyses would help clarify how the location and magnitude of SLH emission sources influence atmospheric responses and would provide a stronger evidence base to inform the sustainable development of seaweed farming in regions with lower potential atmospheric and climate impacts.

Finally, it is important to note that, despite the uncertainties outlined above, the ozone impacts estimated in this study are likely conservative. This aspect is discussed further in the "Conclusions and Sectoral Implications for Seaweed Farming" section of the main manuscript.

References

1. Duarte, C. M., Bruhn, A. & Krause-Jensen, D. A seaweed aquaculture imperative to meet global sustainability targets. *Nature Sustainability 2021 5:3* **5**, 185–193 (2022).
2. van den Burg, S., Koch, S., Raoult, J., Tsvetkov, B. & Selnes, T. Time to Include Blue Carbon from Seaweed in Voluntary Carbon Removal Certification. *EuroChoices* **22**, 13–19 (2023).
3. Saiz-Lopez, A. *et al.* The influence of short-lived halogens on atmospheric chemistry and climate. *Nature 2025 648:8093* **648**, 289–299 (2025).
4. Keng, F. S. L. *et al.* The emission of volatile halocarbons by seaweeds and their response towards environmental changes. *J. Appl. Phycol.* **32**, 1377–1394 (2020).
5. Fernandez, R. P. *et al.* Short-Lived Halogen Sources and Chemistry in the Community Earth System Model v2 (CESM2-SLH). *EGUsphere* 1–65 (2025) doi:10.5194/egusphere-2025-3250.
6. Krause-Jensen, D. & Duarte, C. M. Substantial role of macroalgae in marine carbon sequestration. *Nature Geoscience 2016 9:10* **9**, 737–742 (2016).
7. Pessarrodona, A. *et al.* Long-Term Stability of Marine Forests Facing Moderate Gradual Warming in a Remote Biodiversity Hotspot. *Divers. Distrib.* **30**, e13933 (2024).
8. James, C., Layton, C., Hurd, C. L. & Britton, D. The endemic kelp Lessonia corrugata is being pushed above its thermal limits in an ocean warming hotspot. *J. Phycol.* **60**, 503–516 (2024).
9. Filbee-Dexter, K. *et al.* Carbon export from seaweed forests to deep ocean sinks. *Nature Geoscience 2024 17:6* **17**, 552–559 (2024).
10. Khan, N., Sudhakar, K. & Mamat, R. Macroalgae farming for sustainable future: Navigating opportunities and driving innovation. *Heliyon* **10**, e28208 (2024).
11. Yong, W. T. L., Thien, V. Y., Rupert, R. & Rodrigues, K. F. Seaweed: A potential climate change solution. *Renewable and Sustainable Energy Reviews* **159**, 112222 (2022).

12. Spillias, S. *et al.* The empirical evidence for the social-ecological impacts of seaweed farming. *PLOS Sustainability and Transformation* **2**, e0000042 (2023).
13. THE 17 GOALS | Sustainable Development. https://sdgs.un.org/goals.
14. Alemañ, A. E., Robledo, D. & Hayashi, L. Development of seaweed cultivation in Latin America: current trends and future prospects. *Phycologia* **58**, 462–471 (2019).
15. Blikra, M. J. *et al.* Seaweed products for the future: Using current tools to develop a sustainable food industry. *Trends Food Sci. Technol.* **118**, 765–776 (2021).
16. Choudhary, B., Chauhan, O. P. & Mishra, A. Edible Seaweeds: A Potential Novel Source of Bioactive Metabolites and Nutraceuticals With Human Health Benefits. *Front. Mar. Sci.* **8**, 740054 (2021).
17. Jueterbock, A. *et al.* Roadmap to sustainably develop the European seaweed industry. *npj Ocean Sustainability 2025 4:1* **4**, 22- (2025).
18. Stévant, P., Rebours, C. & Chapman, A. Seaweed aquaculture in Norway: recent industrial developments and future perspectives. *Aquaculture International 2017 25:4* **25**, 1373–1390 (2017).
19. World Bank. 2023. Global Seaweed: New and Emerging Markets Report, 2023. *Global Seaweed: New and Emerging Markets Report, 2023* https://doi.org/10.1596/40187 (2023) doi:10.1596/40187.
20. Commercial Seaweed Market Size, Share, Forecast, 2034. https://www.fortunebusinessinsights.com/industry-reports/commercial-seaweed-market-100077.
21. Duarte, C. M. *et al.* Global estimates of the extent and production of macroalgal forests. *Global Ecology and Biogeography* **31**, 1422–1439 (2022).
22. Wear, B., O'Connor, N. E., Schmid, M. J. & Jackson, M. C. What does the future look like for kelp when facing multiple stressors? *Ecol. Evol.* **13**, e10203 (2023).
23. Assis, J., Fragkopoulou, E., Gouvêa, L., Araújo, M. B. & Serrão, E. A. Kelp forest diversity under projected end-of-century climate change. *Divers. Distrib.* **30**, e13837 (2024).
24. Kumagai, N. H. *et al.* Ocean currents and herbivory drive macroalgae-to-coral community shift under climate warming. *Proc. Natl. Acad. Sci. U. S. A.* **115**, 8990–8995 (2018).
25. Froehlich, H. E., Afflerbach, J. C., Frazier, M. & Halpern, B. S. Blue Growth Potential to Mitigate Climate Change through Seaweed Offsetting. *Current Biology* **29**, 3087-3093.e3 (2019).
26. Arzeno-Soltero, I. B. *et al.* Large global variations in the carbon dioxide removal potential of seaweed farming due to biophysical constraints. *Communications Earth & Environment 2023 4:1* **4**, 185- (2023).
27. Spillias, S. *et al.* Reducing global land-use pressures with seaweed farming. *Nature Sustainability 2023 6:4* **6**, 380–390 (2023).
28. Bhuyan, M. S. Ecological risks associated with seaweed cultivation and identifying risk minimization approaches. *Algal Res.* **69**, 102967 (2023).
29. Campbell, I. *et al.* The environmental risks associated with the development of seaweed farming in Europe - prioritizing key knowledge gaps. *Front. Mar. Sci.* **6**, 379461 (2019).
30. Leedham, E. C. *et al.* Emission of atmospherically significant halocarbons by naturally occurring and farmed tropical macroalgae. *Biogeosciences* **10**, 3615–3633 (2013).
31. Mithoo-Singh, P. K. *et al.* Halocarbon emissions by selected tropical seaweeds: Species-specific and compoundspecific responses under changing pH. *PeerJ* **2017**, e2918 (2017).
32. Quack, B. & Wallace, D. W. R. Air-sea flux of bromoform: Controls, rates, and implications. *Global Biogeochem. Cycles* **17**, (2003).

33. Mtolera, M. S. P. *et al.* Stress-induced production of volatile halogenated organic compounds in Eucheuma denticulatum (Rhodophyta) caused by elevated pH and high light intensities. *Eur. J. Phycol.* **31**, 89–95 (1996).
34. Jia, Y., Quack, B., Kinley, R. D., Pisso, I. & Tegtmeier, S. Potential environmental impact of bromoform from Asparagopsis farming in Australia. *Atmos. Chem. Phys.* **22**, 7631–7646 (2022).
35. Tegtmeier, S. *et al.* Oceanic bromoform emissions weighted by their ozone depletion potential. *Atmos. Chem. Phys.* **15**, 13647–13663 (2015).
36. Iglesias-Suarez, F. *et al.* Natural halogens buffer tropospheric ozone in a changing climate. *Nature Climate Change 2020 10:2* **10**, 147–154 (2020).
37. Roozitalab, B. *et al.* Impacts of Socio-Economic Development Scenarios on Long-Term Oceanic Emissions and Abundances of Atmospheric Bromoform and Dibromomethane. *Journal of Geophysical Research: Atmospheres* **130**, e2025JD044790 (2025).
38. Saiz-Lopez, A. *et al.* Natural short-lived halogens exert an indirect cooling effect on climate. *Nature 2023 618:7967* **618**, 967–973 (2023).
39. Yang, X. *et al.* How sensitive is the recovery of stratospheric ozone to changes in concentrations of very short-lived bromocarbons? *Atmos. Chem. Phys.* **14**, 10431–10438 (2014).
40. Fernandez, R. P., Kinnison, D. E., Lamarque, J. F., Tilmes, S. & Saiz-Lopez, A. Impact of biogenic very short-lived bromine on the Antarctic ozone hole during the 21st century. *Atmos. Chem. Phys.* **17**, 1673–1688 (2017).
41. Hossaini, R. *et al.* A multi-model intercomparison of halogenated very short-lived substances (TransCom-VSLS): Linking oceanic emissions and tropospheric transport for a reconciled estimate of the stratospheric source gas injection of bromine. *Atmos. Chem. Phys.* **16**, 9163–9187 (2016).
42. Villamayor, J. *et al.* Very short-lived halogens amplify ozone depletion trends in the tropical lower stratosphere. *Nature Climate Change 2023 13:6* **13**, 554–560 (2023).
43. WMO. World Meteorological Organization, 'Scientific Assessment of Ozone Depletion: 2022' (Ozone Research and Monitoring-GAW Rep. 278). *Geneva, Switzerland* https://www.csl.noaa.gov/assessments/ozone/2022 (2022).
44. Newman, P. A. *et al.* What would have happened to the ozone layer if chlorofluorocarbons (CFCs) had not been regulated? *Atmos. Chem. Phys* **9**, (2009).
45. Madronich, S. *et al.* Continuing benefits of the Montreal Protocol and protection of the stratospheric ozone layer for human health and the environment. *Photochemical & Photobiological Sciences 2024 23:6* **23**, 1087–1115 (2024).
46. Bernhard, G. H. *et al.* Stratospheric ozone, UV radiation, and climate interactions. *Photochemical & Photobiological Sciences 2023 22:5* **22**, 937–989 (2023).
47. Chipperfield, M. P. *et al.* Quantifying the ozone and ultraviolet benefits already achieved by the Montreal Protocol. *Nature Communications 2015 6:1* **6**, 7233- (2015).
48. Hossaini, R. *et al.* Efficiency of short-lived halogens at influencing climate through depletion of stratospheric ozone. *Nature Geoscience 2014 8:3* **8**, 186–190 (2015).
49. Farman, J. C., Gardiner, B. G. & Shanklin, J. D. Large losses of total ozone in Antarctica reveal seasonal ClOx/NOx interaction. *Nature 1985 315:6016* **315**, 207–210 (1985).
50. Solomon, S., Garcia, R. R., Rowland, F. S. & Wuebbles, D. J. On the depletion of Antarctic ozone. *Nature 1986 321:6072* **321**, 755–758 (1986).
51. Solomon, S. *et al.* Emergence of healing in the Antarctic ozone layer. *Science (1979).* **353**, 269–274 (2016).

52. Chipperfield, M. P. *et al.* Detecting recovery of the stratospheric ozone layer. *Nature 2017 549:7671* **549**, 211–218 (2017).
53. Wang, P. *et al.* Fingerprinting the recovery of Antarctic ozone. *Nature 2025 639:8055* **639**, 646–651 (2025).
54. Montzka, S. A. *et al.* Ozone-depleting substances (ODSs) and related chemicals (chapter 1). *Geneva, Switzerland* (2011).
55. Ordóñez, C. *et al.* Bromine and iodine chemistry in a global chemistry-climate model: Description and evaluation of very short-lived oceanic sources. *Atmos. Chem. Phys.* **12**, 1423–1447 (2012).
56. FAO. 2024. FAO Fisheries and Aquaculture - FishStatJ - Software for Fishery and Aquaculture Statistical Time Series. In: FAO Fisheries and Aquaculture Division [online]. https://www.fao.org/fishery/en/knowledgebase/150.
57. WMO. World Meteorological Organization, 'Scientific Assessment of Ozone Depletion: 2018' (Global Ozone Research and Monitoring Project Rep. 58). *Geneva, Switzerland* (2018).
58. Tegtmeier, S., Atlas, E., Quack, B., Ziska, F. & Krüger, K. Variability and past long-term changes of brominated very short-lived substances at the tropical tropopause. *Atmos. Chem. Phys.* **20**, 7103–7123 (2020).
59. Jesswein, M. *et al.* Global seasonal distribution of CH2Br2 and CHBr3 in the upper troposphere and lower stratosphere. *Atmos. Chem. Phys.* **22**, 15049–15070 (2022).
60. Matsumura, Y. Nutrition trends in Japan. *Asia Pac. J. Clin. Nutr.* **10**, S40–S47 (2001).
61. Keeble, J. *et al.* Evaluating stratospheric ozone and water vapour changes in CMIP6 models from 1850 to 2100. *Atmos. Chem. Phys.* **21**, 5015–5061 (2021).
62. Riese, M. *et al.* Impact of uncertainties in atmospheric mixing on simulated UTLS composition and related radiative effects. *Journal of Geophysical Research Atmospheres* **117**, 16305 (2012).
63. Zhu, P. *et al.* Commercial cultivation, industrial application, and potential halocarbon biosynthesis pathway of Asparagopsis sp. *Algal Res.* **56**, 102319 (2021).
64. Taenzer, L., Toth, G. & Hansel, C. M. Assessment of hydrogen peroxide as a bioindicator of stress in seaweed aquaculture. *Scientific Reports 2024 14:1* **14**, 1956- (2024).
65. Mackintosh, A. L., Hill, G. G., Costello, M. J. & Assis, J. No significant projected climate change effects on the geographic ranges of marine aquaculture species under the sustainable scenario (SSP 1-1.9, 1.5°C warming). *npj Ocean Sustainability 2025 5:1* **5**, 7- (2025).
66. Buschmann, A. H. *et al.* Seaweed production: overview of the global state of exploitation, farming and emerging research activity. *Eur. J. Phycol.* **52**, 391–406 (2017).
67. Lester, S. E. *et al.* Diverse state-level marine aquaculture policy in the United States: Opportunities and barriers for industry development. *Rev. Aquac.* **14**, 890–906 (2022).
68. Ruff, E. O., Gentry, R. R. & Lester, S. E. Understanding the role of socioeconomic and governance conditions in country-level marine aquaculture production. *Environmental Research Letters* **15**, 1040a8 (2020).
69. Filbee-Dexter, K. *et al.* Sea Ice and Substratum Shape Extensive Kelp Forests in the Canadian Arctic. *Front. Mar. Sci.* **9**, 754074 (2022).
70. Stekoll, M. S., Deysher, L. E. & Hess, M. A remote sensing approach to estimating harvestable kelp biomass. *Journal of Applied Phycology 2006 18:3* **18**, 323–334 (2006).
71. Giraldo-Ospina, A., Bell, T., Carr, M. H. & Caselle, J. E. Drivers of spatiotemporal variability in a marine foundation species. *Ecological Applications* **35**, e3092 (2025).

72. Wu, J., Keller, D. P. & Oschlies, A. Carbon dioxide removal via macroalgae open-ocean mariculture and sinking: an Earth system modeling study. *Earth System Dynamics* **14**, 185–221 (2023).
73. Klick, S. The release of volatile halocarbons to seawater by untreated and heavy metal exposed samples of the brown seaweed Fucus Vesiculosus. *Mar. Chem.* **42**, 211–221 (1993).
74. Manley, S. L. & Dastoor, M. N. Methyl iodide (CH3I) production by kelp and associated microbes. *Mar. Biol.* **98**, 477–482 (1988).
75. Manley, S. L., Goodwin, K. & North, W. J. Laboratory production of bromoform, methylene bromide, and methyl iodide by macroalgae and distribution in nearshore southern California waters. *Limnol. Oceanogr.* **37**, 1652–1659 (1992).
76. Manley, S. L. & Dastoor, M. N. Methyl halide (CH3X) production from the giant kelp, Macrocystis, and estimates of global CH3X production by kelp. *Limnol. Oceanogr.* **32**, 709–715 (1987).
77. Goodwin, K. D., North, W. J. & Lidstrom, M. E. Production of bromoform and dibromomethane by Giant Kelp: Factors affecting release and comparison to anthropogenic bromine sources. *Limnol. Oceanogr.* **42**, 1725–1734 (1997).
78. Laturnus, F. Marine macroalgae in polar regions as natural sources for volatile organohalogens. *Environmental Science and Pollution Research 2001 8:2* **8**, 103–108 (2001).
79. Pedersen, M., Collen, J., Abrahamsson, K. & Ekdahl, A. Production of halocarbons from seaweeds: An oxidative stress reaction? *Sci. Mar.* **60**, 257–263 (1996).
80. Bravo-Linares, C. M., Mudge, S. M. & Loyola-Sepulveda, R. H. Production of volatile organic compounds (VOCs) by temperate macroalgae: The use of Solid Phase Microextraction (SPME) coupled to GC-MS as method of analysis. *Journal of the Chilean Chemical Society* **55**, 227–232 (2010).
81. Baker, J. M. *et al.* Emissions of CH3Br, organochlorines, and organoiodines from temperate macroalgae. *Chemosphere - Global Change Science* **3**, 93–106 (2001).
82. Gschwend, P. M., MacFarlane, J. K. & Newman, K. A. Volatile halogenated organic compounds released to seawater from temperate marine macroalgae. *Science (1979).* **227**, 1033–1035 (1985).
83. Nightingale, P. D., Malin, G. & Liss, P. S. Production of chloroform and other low molecular-weight halocarbons by some species of macroalgae. *Limnol. Oceanogr.* **40**, 680–689 (1995).
84. Carpenter, L. J. & Liss, P. S. On temperate sources of bromoform and other reactive organic bromine gases. *Journal of Geophysical Research Atmospheres* **105**, 20539–20547 (2000).
85. Paul, N. A., De Nys, R. & Steinberg, P. D. Chemical defence against bacteria in the red alga Asparagopsis armata: linking structure with function. *Mar. Ecol. Prog. Ser.* **306**, 87–101 (2006).
86. Marshall, R. A., Harper, D. B., McRoberts, W. C. & Dring, M. J. Volatile bromocarbons produced by Falkenbergia stages of Asparagopsis spp. (Rhodophyta). *Limnol. Oceanogr.* **44**, 1348–1352 (1999).
87. Matsuda, R. *et al.* Preferential Expression of a Bromoperoxidase in Sporophytes of a Red Alga, Pyropia yezoensis. *Marine Biotechnology 2014 17:2* **17**, 199–210 (2014).
88. Ekdahl, A., Pedersén, M. & Abrahamsson, K. A study of the diurnal variation of biogenic volatile halocarbons. *Mar. Chem.* **63**, 1–8 (1998).

89. Weinberger, F. *et al.* Different regulation of haloperoxidation during agar oligosaccharide-activated defence mechanisms in two related red algae, Gracilaria sp. and Gracilaria chilensis. *J. Exp. Bot.* **58**, 4365–4372 (2007).
90. Keng, F. S. L. *et al.* Volatile halocarbon emissions by three tropical brown seaweeds under different irradiances. *Journal of Applied Phycology 2013 25:5* **25**, 1377–1386 (2013).
91. Fernandez, R. P. *et al.* Intercomparison Between Surrogate, Explicit, and Full Treatments of VSL Bromine Chemistry Within the CAM-Chem Chemistry-Climate Model. *Geophys. Res. Lett.* **48**, e2020GL091125 (2021).
92. Keng, F. S. L. *et al.* Emission of volatile halocarbons from the farming of commercially important tropical seaweeds. *Journal of Applied Phycology 2023 35:6* **35**, 3007–3020 (2023).
93. Glasson, C. R. K. *et al.* Benefits and risks of including the bromoform containing seaweed Asparagopsis in feed for the reduction of methane production from ruminants. *Algal Res.* **64**, 102673 (2022).
94. Gettelman, A. *et al.* The Whole Atmosphere Community Climate Model Version 6 (WACCM6). *Journal of Geophysical Research: Atmospheres* **124**, 12380–12403 (2019).
95. Smith, R. *et al.* The Parallel Ocean Program (POP) Reference Manual Ocean Component of the Community Climate System Model (CCSM) and Community Earth System Model (CESM) 1. (2010).
96. Emmons, L. K. *et al.* The Chemistry Mechanism in the Community Earth System Model Version 2 (CESM2). *J. Adv. Model. Earth Syst.* **12**, e2019MS001882 (2020).
97. Meinshausen, M. *et al.* The shared socio-economic pathway (SSP) greenhouse gas concentrations and their extensions to 2500. *Geosci. Model Dev.* **13**, 3571–3605 (2020).
98. Prados-Roman, C. *et al.* Iodine oxide in the global marine boundary layer. *Atmos. Chem. Phys.* **15**, 583–593 (2015).
99. Fernandez, R. P., Salawitch, R. J., Kinnison, D. E., Lamarque, J. F. & Saiz-Lopez, A. Bromine partitioning in the tropical tropopause layer: Implications for stratospheric injection. *Atmos. Chem. Phys.* **14**, 13391–13410 (2014).
100. Hossaini, R. *et al.* Recent Trends in Stratospheric Chlorine From Very Short-Lived Substances. *Journal of Geophysical Research: Atmospheres* **124**, 2318–2335 (2019).
101. Claxton, T. *et al.* A Synthesis Inversion to Constrain Global Emissions of Two Very Short Lived Chlorocarbons: Dichloromethane, and Perchloroethylene. *Journal of Geophysical Research: Atmospheres* **125**, e2019JD031818 (2020).
102. Bodeker, G. E. *et al.* A global total column ozone climate data record. *Earth Syst. Sci. Data* **13**, 3885–3906 (2021).

Acknowledgments:

We thank Hansi Singh for initiating this research and for her support during early stages of the project. We thank Lasse Broska for his help in compiling the dataset of seaweed dry-weight to fresh-weight ratios. We thank Douglas Kinnison for helpful discussions on the impact of SLH on the ozone layer. The CESM project is supported primarily by the National Science Foundation (NSF). This material is based on work supported by the National Center for Atmospheric Research, which is a major facility sponsored by the NSF under Cooperative Agreement No. 1852977. Computing and data storage resources, including the Derecho supercomputer

(https://doi.org/10.5065/qx9a-pg09), were provided by the Computational and Information Systems Laboratory (CISL) at NCAR. This research is publication no. 13 of Blue Carbon Canada (www.bluecarboncanda.ca) - a multi-institute research program funded supported by the Natural Sciences and Engineering Research Council of Canada's (NSERC) Alliance partnership grant (grant numbers: ALLRP 571068-21) and the Department of Fisheries and Oceans Canada (DFO) the Department of Fisheries and Oceans Canada (DFO, contract number: UN2021-025). Blue Carbon Canada is endorsed by the United Nations Decade of Ocean Science for Sustainable Development and the Global Ocean Decade Programme for Blue Carbon (https://www.go-bc.co.uk/go-bc-partnerships-1/blue-carbon-canada). The Indian Institute of Tropical Meteorology is funded by the Ministry of Earth Sciences, Government of India.

Funding:

High-Impact Federal Network grant REMATE IF-2023-85161983-APN (Argentine Secretary of Science)

Natural Sciences and Engineering Research Council of Canada's Alliance partnership grant ALLRP 571068-21 (JV(1), JM, JKB)

Department of Fisheries and Oceans Canada contract number: UN2021-025 (JV(1), JM, JKB)

Mitacs Accelerate grant numbers IT28407 and IT45250 with partner support from Oceans North and World Wildlife fund (JM)

Author contributions:

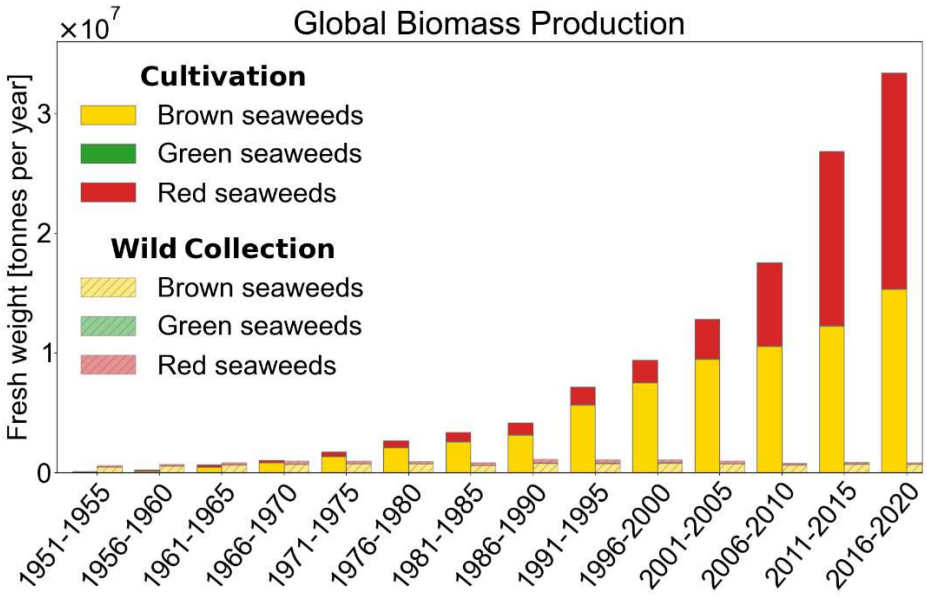
Conceptualization was carried out by J.V. (1), J.V. (2), J.M., J.K.B., A.S.M. and A.S.L. Methodology was developed by J.V. (1), J.V. (2), R.P.F., J.M., C.A.C., A.S.M. and A.S.L. Investigation was conducted by J.V. (1), J.V. (2), R.P.F., J.M., C.A.C., M.S., A.S.M. and A.S.L. Visualization was performed by J.V. (1), J.V. (2), R.P.F., J.M. and M.S. Funding acquisition was carried out by J.K.B., A.S.M. and A.S.L., and project administration by J.K.B. and A.S.L. The original draft was written by J.V. (1) and J.V. (2), who contributed equally to this work. All authors (J.V. (1), J.V. (2), R.P.F., J.M., C.A.C., M.G., M.S., J.K.B., A.S.M. and A.S.L.) contributed to the review and editing of the manuscript.

Competing interests:

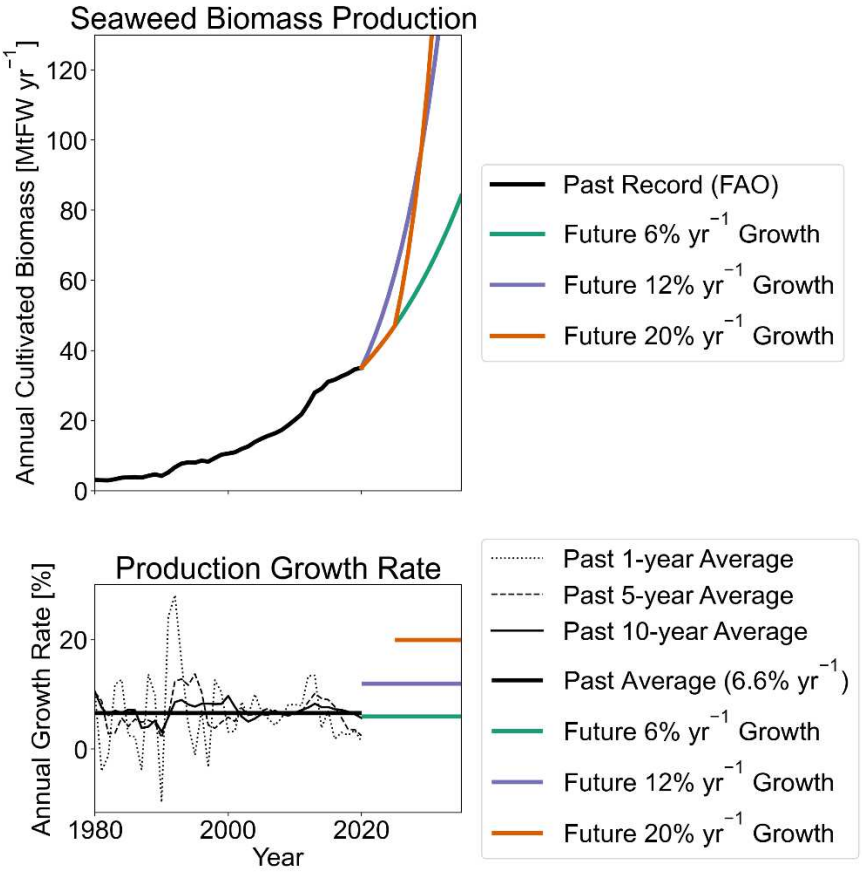
The authors declare no competing interests.

Data and materials availability:

The data underlying this study, along with the code used to generate the emissions data and conduct the analyses, will be deposited in Borealis under the Blue Carbon Canada Dataverse (https://borealisdata.ca/dataverse/bluecarboncanada) and made publicly available upon publication. There are no restrictions on data availability (no MTAs apply).

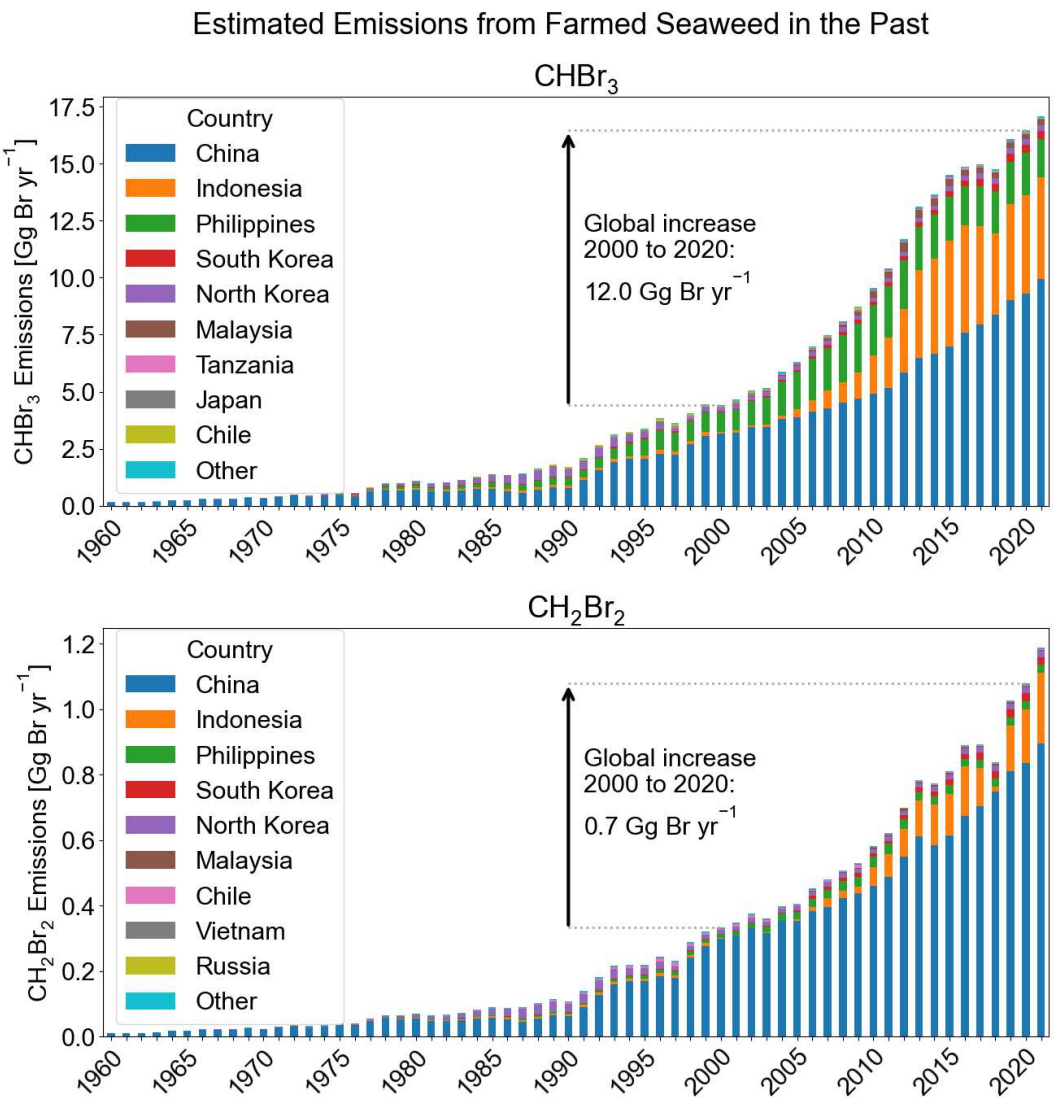


Extended Data Fig. 1. The 5-year means from 1951 to 2020 indicate that global seaweed production has increased significantly over past decades [56]. While the wild collection of natural seaweed has remained at a low amount, cultivation is following accelerated growth with similar contributions from red (Rhodophyta; mostly *Eucheuma*, *Kappaphycus*) and brown (Phaeophyceae; mostly *Saccharina*) seaweed groups. Green seaweed (Chlorophyta) is barely contributing to global production. For comparison, in 2023, about 98% of commercial seaweeds were farmed and only 2% were collected wild.

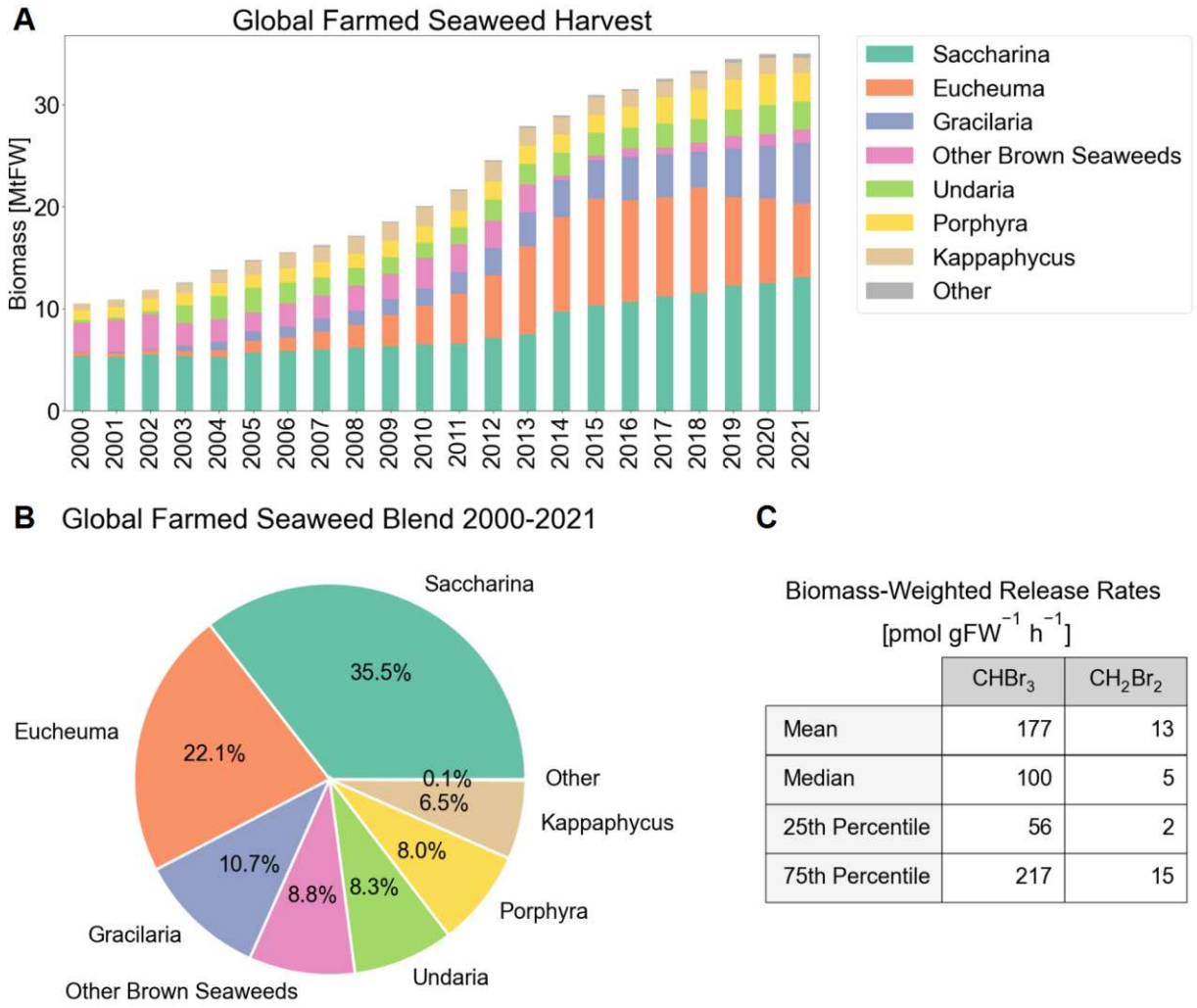


916

917 **Extended Data Fig. 2.** Past (FAO-reported[56]) and future (scenario-based) seaweed cultivation
918 biomass (top) and associated annual growth rates (bottom).

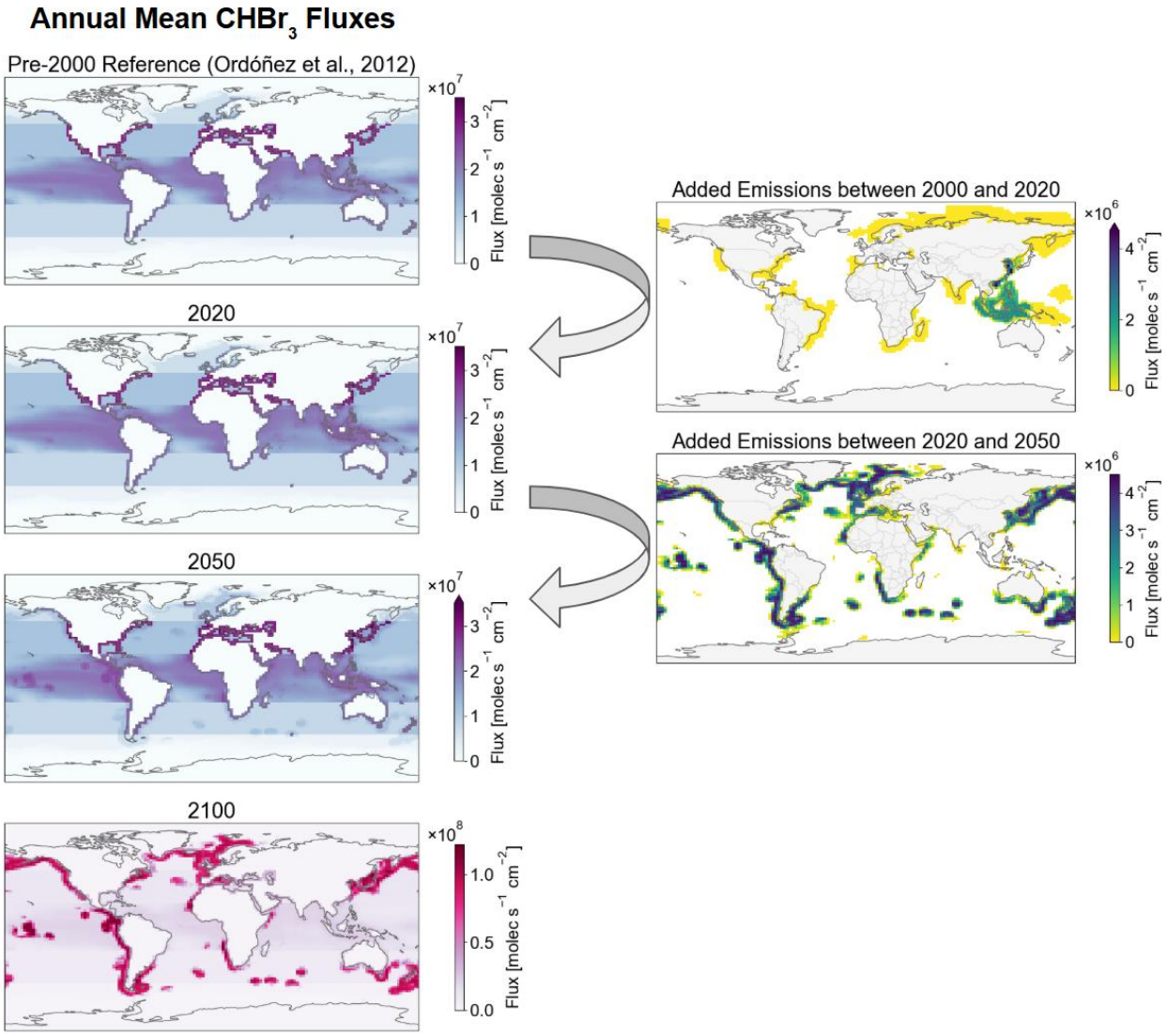


Extended Data Fig. 3. Past emissions of $CHBr_3$ (top) and CH_2Br_2 (bottom) from seaweed aquaculture in units of gigagrams bromine per year (Gg Br yr^{-1}). Values are estimated using FAO-reported biomass[56] and upper range release rate estimates for the seaweeds cultivated by each country. The individual contributions of the nine countries with highest emissions in 2020 are stacked in ranking order.

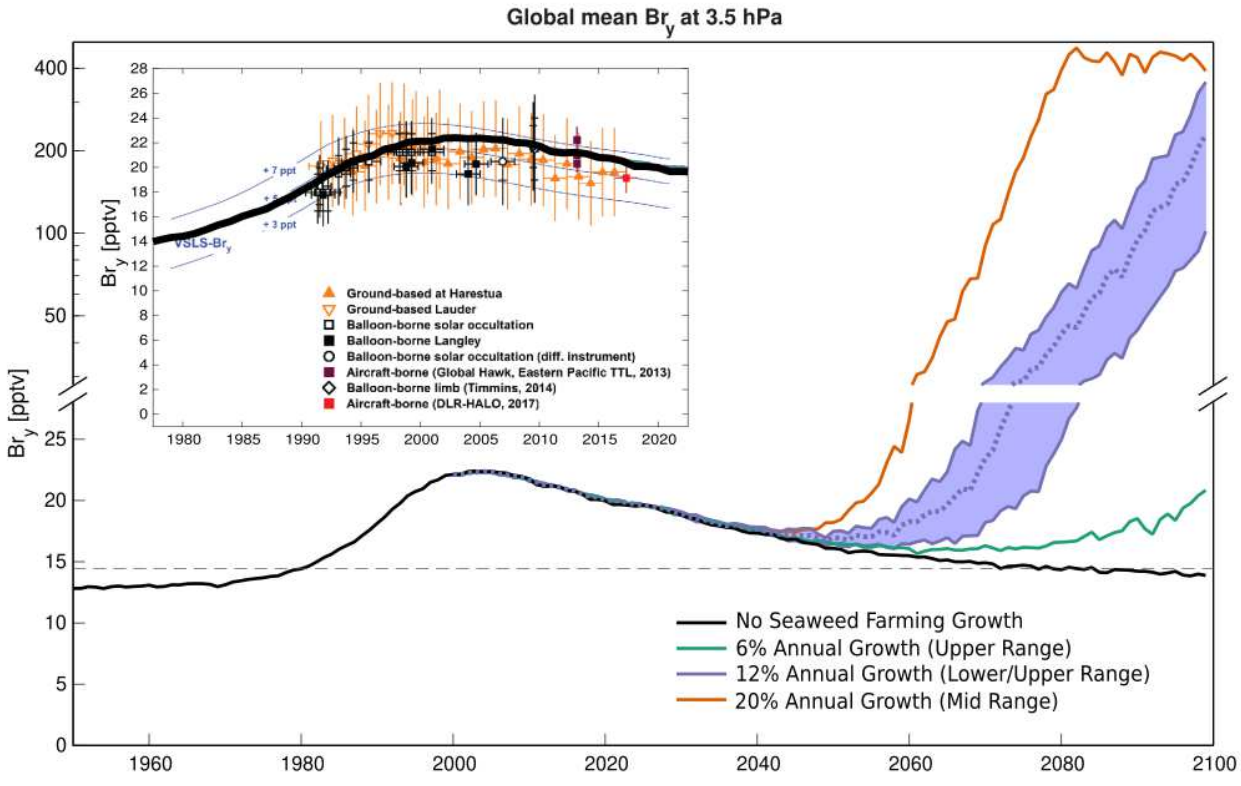


	$CHBr_3$	CH_2Br_2
Mean	177	13
Median	100	5
25th Percentile	56	2
75th Percentile	217	15

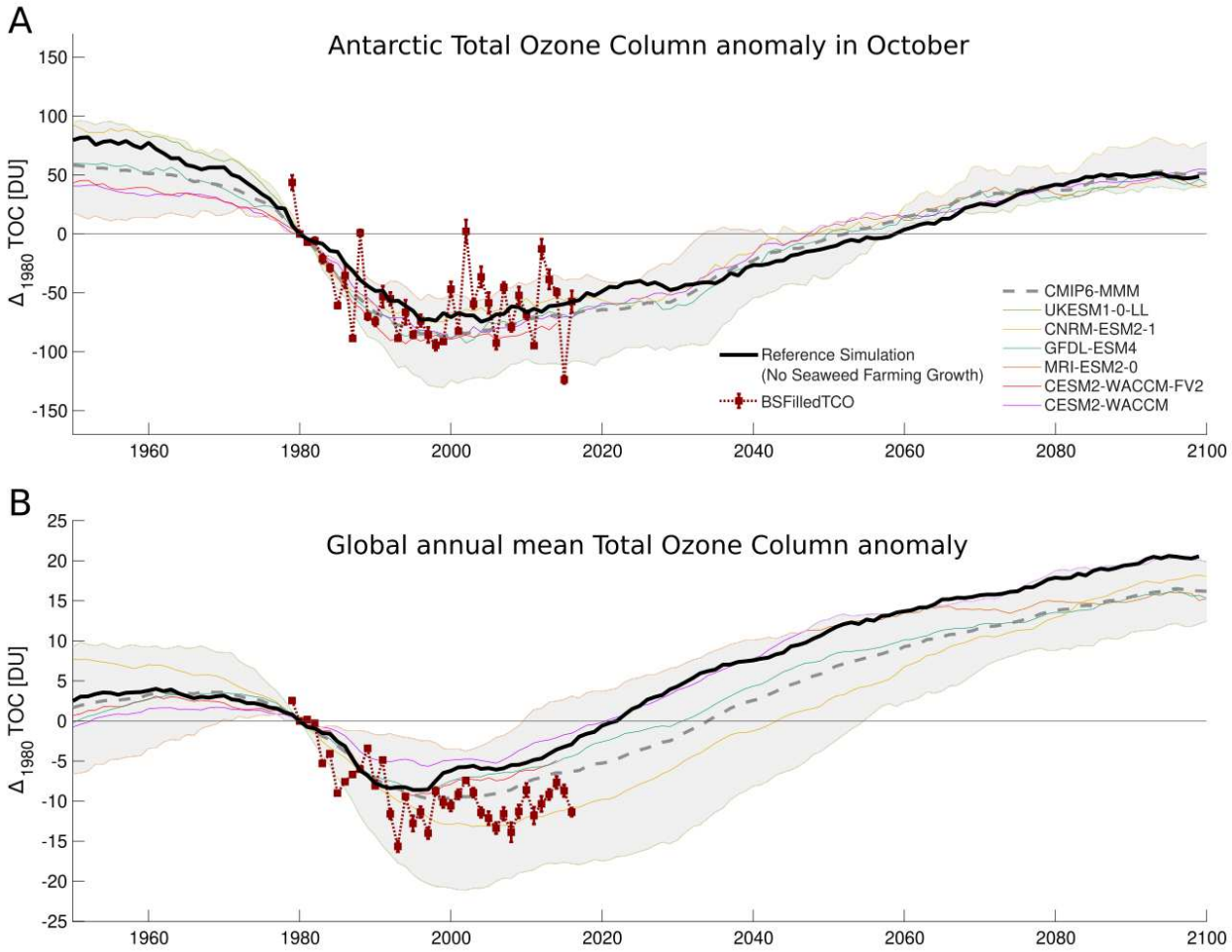
Extended Data Fig. 4. (**A**) The amount and composition of globally farmed seaweed have changed over past decades. (**B**) The future seaweed blend is approximated by the past 22-year average and held constant. (**C**) This past-average seaweed blend is the basis for the estimated future range of release rates in this study. Since the global seaweed composition evolves (Extended Data Fig. 3) and SLH release rates vary widely among seaweed species (Fig. 1), the assumption of a constant seaweed blend and release-rate range is one source of uncertainty in this study.



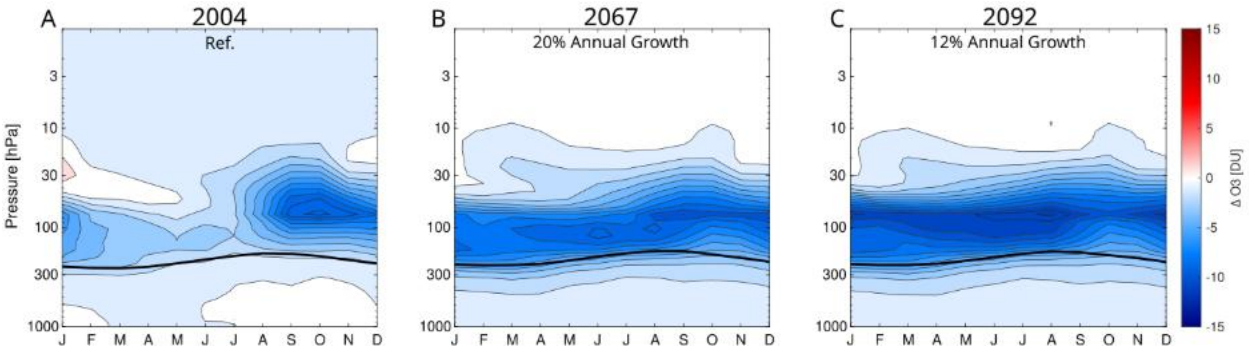
Extended Data Fig. 5. (Left column) Time slices of $CHBr_3$ fluxes used as input to the CESM2-SLH model. The input data combines reference emissions from Ordóñez et al.[55] with additional seaweed-derived emissions (right column): recorded increases based on FAO data from 2000-2020 [56], and projections following the 6% yr^{-1} growth scenario from 2020-2100 assuming the lower-range estimate of $CHBr_3$ release rates. Note that color scales differ between panels due to large variations in maximum flux values.



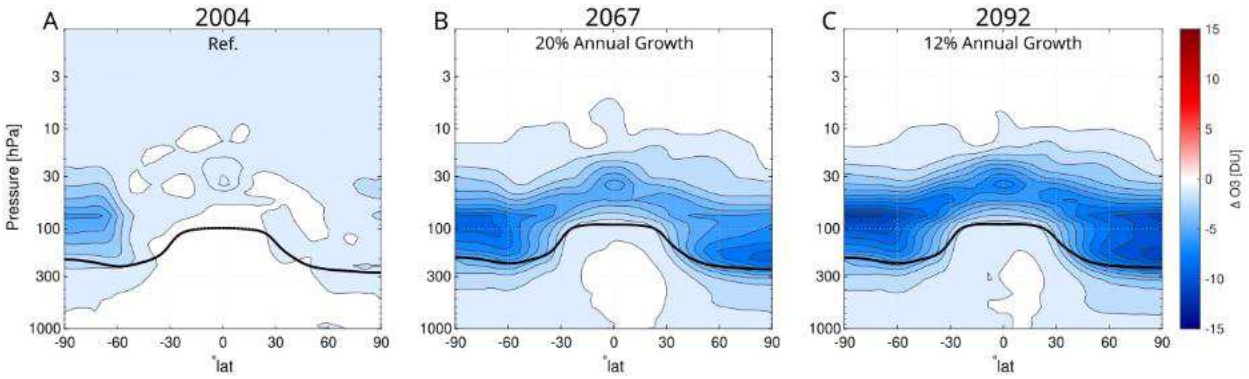
Extended Data Fig. 6. Global-mean stratospheric inorganic bromine (Br_y in pptv) at the top of the stratosphere (3.5 hPa) for the different seaweed-farming scenarios considered in this work (see legend). Note that the y-axis is split at 30 pptv, with a linear scale below the break and a logarithmic scale above. The inset shows a comparison with published equivalent Br_y reported estimates and observations from multiple sources (see inset legend), with our simulated results (black line) overlaid on an adapted version of Figure 1-14a from WMO´s Scientific Assessment of Ozone Depletion: 2022[43].



Extended Data Fig. 7. Validation of the reference simulation (no seaweed farming growth; extended into the future following the SSP3-7.0 scenario) against observations and selected CMIP6 models (see legend). Δ_{1980} TOC represents the total ozone column anomalies relative to 1980, averaged over (**A**) Antarctica (90º - 60º S) in October and (**B**) the global annual mean. Observational estimates from BSFilledTCO-v3.4 are shown for the period 1979–2016, with error bars indicating ±2 standard deviations. Colored lines show individual CMIP6 models with interactive chemistry from previous assessments[61]: one ensemble member per model is shown for the historical simulation (to 2014) continued under SSP3-7.0 (2015–2100), except for CESM2-WACCM-FV2. The grey shading denotes the full range spanned by the CMIP6 models, and the grey dashed line denotes the CMIP6 multi-model mean (CMIP6-MMM). All model time series are smoothed with an 11-year centered running mean; observations are shown without filtering.



Extended Data Fig. 8. Annual cycle of the vertical distribution of Antarctic partial ozone column anomalies relative to 1980 averaged over 90º - 60º S. Displayed are the 11-year mean anomalies centered on (**A**) 2004 in the reference simulation, (**B**) 2067 in the median 20% yr^{-1} growth scenario, and (**C**) 2092 in the ensemble-mean 12% yr^{-1} growth scenario. The thick black line denotes the mean tropopause height.



968

969 **Extended Data Fig. 9**. Vertical distribution of the zonal mean partial ozone column anomalies
970 relative to 1980. Displayed are the 11-year mean anomalies centered on (**A**) 2004 in the reference
971 simulation, (**B**) 2067 in the median 20% yr^{-1} growth scenario, and (**C**) 2092 in the ensemble-mean
972 12% yr^{-1} growth scenario. The thick black line denotes the mean tropopause height.

973